Trimerisation of the Cationic Fragments $[(\eta\text{-ring})M(Aa)]^+$ ((η-ring) M = (η^5-C_5Me_5)Rh, (η^5-C_5Me_5)Ir, (η^6-*p*-MeC_6H_4*i*Pr)Ru; Aa = α-amino acidate) with Chiral Self-Recognition: Synthesis, Characterisation, Solution Studies and Catalytic Reactions of the Trimers $[\{(\eta\text{-ring})M(Aa)\}_3](BF_4)_3$

Daniel Carmona,*[a] Fernando J. Lahoz,[a] Reinaldo Atencio,[a] Luis A. Oro,*[a] M. Pilar Lamata,[b] Fernando Viguri,[b] Emilio San José,[b] Cristina Vega,[b] Josefa Reyes,[c] Ferenc Joó,*[d] and Ágnes Kathó[d]

Abstract: The mononuclear neutral chlorides $[(\eta\text{-ring})M(Aa)Cl]$ ((η-ring)-M = (η^5-C_5Me_5)Rh, (η^5-C_5Me_5)Ir, (η^6-*p*-MeC_6H_4*i*Pr)Ru; Aa = α-amino acidate) were treated with $AgBF_4$ to yield the corresponding new chiral trimers $[\{(\eta\text{-ring})M(Aa)\}_3](BF_4)_3$. Compounds $[\{(\eta^5\text{-}C_5Me_5)Ir(Ala)\}_3](BF_4)_3$ (**1b**) and $[\{(\eta^6\text{-}p\text{-}MeC_6H_4iPr)Ru(L\text{-}Pro)\}_3](BF_4)_3$ (**6c**) were characterised by X-ray diffraction. Trimerisation takes place by chiral self-recognition: the trimers $R_MR_MR_M$ (ρ isomer) or $S_MS_MS_M$ (σ isomer), which have equal configuration at the metal centre, were the only diastereomers detected. In solution, a diastereomerisation process between both isomers occurs, where the equilibrium constant depends on the solvent, amino acidate, and metal. The different localisation of the polar groups (NH or NH_2 moieties) on the molecular surface of the two diastereomers (ρ and σ) provides a qualitative explanation for the different diastereomer stability observed in solution. The new chiral trimers catalyse the reduction of unsaturated aldehydes to unsaturated alcohols by hydrogen transfer from aqueous sodium formate and the reduction of acetophenone by hydrogen transfer from 2-propanol with up to 75 % *ee*.

Keywords: amino acids · asymmetric catalysis · iridium · rhodium · ruthenium

Introduction

The previously reported[1] chiral-at-metal α-amino acidate chloride complexes $[(\eta\text{-ring})M(Aa)Cl]$ ((η-ring)M = (η^5-C_5Me_5)Rh, (η^5-C_5Me_5)Ir, (η^6-*p*-MeC_6H_4*i*Pr)Ru; Aa = α-amino acidate) act as ionic conductors in polar solvents such as methanol or water, with molar conductances greater than 60 $ohm^{-1}cm^2mol^{-1}$ in water.[1b] The ^1H NMR spectra of the ruthenium chloride compounds $[(\eta^6\text{-}p\text{-}MeC_6H_4iPr)Ru(Aa)Cl]$ (Aa = Ala, L-Pro) in D_2O were affected by the presence of LiCl. This behaviour was explained by the assumption of a reversible ionisation of the chloride ligand from the two possible epimers at the metal centre.[1b, 2] However, the ^1H NMR spectra of the related rhodium and iridium chloride compounds $[(\eta^5\text{-}C_5Me_5)M(Aa)Cl]$ (M = Rh, Ir; Aa = Ala, L-Pro) in the same solvent, showed only one set of resonances which were not affected by the addition of excess lithium salt. Additionally, conductance measurements in water gave values for the slope of the Onsager equation that clearly pointed to a molecular complexity greater than that of univalent electrolytes.[3]

In order to obtain further insights into the actual nature of these complexes in solution, the reaction of a variety of chlorides of the three metals with $AgBF_4$ was carried out, which resulted in the preparation of a family of chiral-at-metal trimers of the general formula $[\{(\eta\text{-ring})M(Aa)\}_3](BF_4)_3$. One member of this family, $[\{(\eta^5\text{-}C_5Me_5)Rh(Phe)\}_3](BF_4)_3$ (Phe =

[a] Dr. D. Carmona, Dr. F. J. Lahoz, Dr. R. Atencio, Prof. L. A. Oro
Departamento de Química Inorgánica
Instituto de Ciencia de Materiales de Aragón
Universidad de Zaragoza-C.S.I.C., 50009 Zaragoza (Spain)
Fax: (+34) 976-761187 or 1143
E-mail: dcarmona@posta.unizar.es

[b] Dr. M. P. Lamata, Dr. F. Viguri, Dr. E. San José, C. Vega
Departamento de Química Inorgánica
Escuela Universitaria de Ingeniería Técnica Industrial
Instituto de Ciencia de Materiales de Aragón
Universidad de Zaragoza-C.S.I.C.
Corona de Aragón 35, E-50009 Zaragoza (Spain)

[c] Dr. J. Reyes
Departamento de Química Inorgánica
Centro Politécnico Superior
Instituto de Ciencia de Materiales de Aragón
Universidad de Zaragoza-C.S.I.C.
María Zambrano s/n, 50015 Zaragoza (Spain)

[d] Prof. F. Joó, Dr. Ágnes Kathó
Institute of Physical Chemistry, Lajos Kossuth University
4010 Debrecen (Hungary)

0947-6539/99/0505-1544 $ 17.50+.50/0 *Chem. Eur. J.* **1999**, *5*, No. 5

phenylalaninate), has been previously prepared by Beck et al.[4]

Herein we report the preparation, characterisation and solution studies of these trimers. The trinuclear nature of the metal complexes together with the complete configurational characterisation of the different diastereomers was confirmed by a single-crystal X-ray diffraction study of two representative complexes and comparative analysis of the ^{1}H NMR and circular dichroism spectra for all synthesised complexes.

Furthermore, investigation of the catalytic properties of the new complexes, together with those of the mononuclear analogues prepared earlier, was undertaken for two equally important reasons. With a few exceptions, these compounds are soluble in water and have the potential for application in aqueous/organic biphasic processes which are the objects of intensive current research.[5] Secondly, the chirality of these complexes, both on the ligand and the metal, could provide the means for asymmetric catalytic transformations.

For our complexes, the retention of chirality during a catalytic reaction requires that the metal bonding of both the arene and amino acidate ligands is maintained. For that reason, reactions which can proceed without the need for simultaneous coordination of three new ligands, were attempted, namely i) reduction of unsaturated aldehydes by hydrogen transfer from aqueous sodium formate and ii) reduction of acetophenone by hydrogen transfer from 2-propanol. In addition, some experiments were also done on olefin isomerisation. Selective reduction of unsaturated carbonyl compounds to unsaturated alcohols[6a] and the stereoselective reduction of ketones[6b,c] are important practical processes and can be effected by several Ru, Rh, and Ir complexes, while the transfer hydrogenation of acetophenone[7] is a standard reaction to characterise the catalytic activity and enantioselectivity of new catalysts.

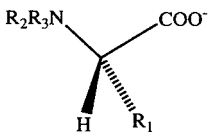

R_1	R_2	R_3	Abbrv.
Me	H	H	Ala
Et	H	H	Abu
i-Pro	H	H	Val
t-Bu	H	H	Tle
Bz	H	H	Phe
$(CH_2)_3$		H	*L*-Pro
$(CH_2)_3$		Me	Me-Pro
$CH_2CHOHCH_2$		H	Hyp

(η-ring)M = (η^5-C_5Me_5)Rh ([Rh]), (η^5-C_5Me_5)Ir ([Ir]), (η^6-*p*-MeC_6H_4*i*-Pr)Ru ([Ru])

Scheme 1. Abbreviations of the amino acidate ligands and metallic fragments. Ala = alaninate; Abu = 2-amino butirate; Val = valinate; Tle = tertleucinate; Phe = phenylalaninate; L-Pro = L-prolinate; Me-Pro = *N*-methyl-L-prolinate; Hyp = 4-hydroxy-L-prolinate.

Results

Synthesis and spectroscopic characterisation: Abbreviations of the amino acidate ligands and metallic fragments are given in Scheme 1. The configuration of the amino acidate is stated for L-Pro (or D-Pro) only; otherwise Aa indicates L-Aa.

The new trimers were prepared, in methanol, in accordance with Equation (1).

$$[(\eta\text{-ring})M(Aa)Cl] + AgBF_4 \rightarrow \tfrac{1}{3}[\{(\eta\text{-ring})M(Aa)\}_3](BF_4)_3 + AgCl \quad (1)$$

Aa = Ala	(η-ring)M = [Rh] **1a**, [Ir] **1b**, [Ru] **1c**
Abu	[Rh] **2a**
Val	[Rh] **3a**, [Ir] **3b**, [Ru] **3c**
Tle	[Rh] **4a**, [Ir] **4b**, [Ru] **4c**
Phe	[Rh] **5a**, [Ir] **5b**, [Ru] **5c**
L-Pro	[Rh] **6a**, [Ir] **6b**, [Ru] **6c**
D-Pro	[Rh] **7a**, [Ir] **7b**, [Ru] **7c**
Me-Pro	[Rh] **8a**, [Ir] **8b**
Hyp	[Rh] **9a**, [Ir] **9b**, [Ru] **9c**

Microanalysis of the isolated solids (see Experimental Section) were consistent with a 1:1:1 ratio of metallic fragment [M], α-amino acidate, and BF_4 anion. The FAB mass spectra showed, in all cases, a peak at the *m/z* ratio calculated for the fragment $[\{(\eta\text{-ring})M(Aa)\}_3(BF_4)_2]^+$, with the appropriate isotopic distribution, along with peaks assignable to di- and monometallic species. Conductance measurements at different concentrations, in acetone or methanol, gave values for the slope in the Onsager equation (see Experimental Section) that pointed to 3:1 electrolytes, although for the ruthenium compounds, this parameter shows very variable values (from 695.1 (**5c**) to 1566.4 (**3c**)).[3, 8] Table 1 contains ^{1}H NMR data for the new compounds. As expected, the ^{1}H NMR spectra of **1b**, **6a** and **6b** in D_2O were identical to those measured in the same solvent, for the parent chlorides $[(\eta^5\text{-}C_5Me_5)Ir(Ala)Cl]$, $[(\eta^5\text{-}C_5Me_5)Rh(L\text{-}Pro)Cl]$, and $[(\eta^5\text{-}C_5Me_5)Ir(L\text{-}Pro)Cl]$, which confirms that complete dissociation of the chloride ligand occurred in water. The IR spectra of solids **1**–**9** showed strong ν(NH) bands in the 3200 cm^{-1} region,[9] the characteristic bands of the uncoordinated BF_4 anion with T_d symmetry,[10] and a very strong ν(CO) absorption at 1530–1590 cm^{-1} that, interestingly, was shifted 35–95 cm^{-1} to lower energies with respect to the parent chlorides. All these data strongly suggested a polymeric formulation involving the COO functionality. In order to elucidate their molecular structure, complexes **1b** and **6c** were studied by X-ray diffraction methods.

Molecular structures of $[\{(\eta^5\text{-}C_5Me_5)Ir(Ala)\}_3](BF_4)_3$ (1b) and $[\{(\eta^6\text{-}p\text{-}MeC_6H_4iPr)Ru(L\text{-}Pro)\}_3](BF_4)_3 \cdot 3CH_3OH$ (6c): The crystalline structures of **1b** and **6c** constitute trimeric cationic complexes $[\{(\eta\text{-ring})M(Aa)\}_3]^{3+}$ with BF_4^- counterions. In the case of **6c**, methanol solvent molecules are also present in the crystals. The trinuclear metal complexes of **1b** and **6c** exhibit analogous molecular structures, with the amino acidate ligands acting in both cases as tridentate bridging groups (Figures 1 and 2). The entire cationic complex of **1b** has crystallographically imposed three-fold symmetry relating the geometrical parameters of the three metal centres, while this symmetry is only apparent in the structure of **6c**. The nitrogen atom and one of the carboxylic oxygen atoms of

Table 1. ^{1}H NMR data[a] for complexes **1**–**9**.

Complex	C_5Me_5	C*H	R_1	NH_2
1b[b]	1.60 (s)	3.95 (m)	1.27 (d, $J=6.9$) (Me)	3.61 (m), 4.74 (d, $J=11.1$)
3a[c]	1.94 (s)	3.03 (m)	0.96 (d, $J=7.1$) (Me), 0.98 (d, $J=7.0$) (Me), 2.34 (m) (CH)	3.93 (m), 4.84 (m)
3b[b]	1.73 (s)	3.55 (m)	1.00 (d, $J=6.9$) (Me), 1.11 (d, $J=7.0$) (Me), 2.20 (m) (CH)	4.20 (m), 4.35 (m)
4a[c]	1.95 (s)	2.51 (dd, $J=11.2$, 5.6)	1.08 (s) (*t*Bu)	4.38 (pt, $J=11.2$), 5.15 (bs)
4b[c]	1.89 (s)	3.14 (dd, $J=10.5$, 6.8)	1.14 (s) (*t*Bu)	4.92 (pt, $J=10.5$), 5.71 (dd, $J=10.5$, 6.8)
5a[c]	1.88 (s)	3.02 (m)	2.9–3.3 (m) (CH_2), 7.2–7.4 (m) (Ph)	4.55(m), 4.8 (m)
5b[c]	1.82 (s)	3.84 (m)	3.02 (dd, $J=14.6$, 10.6) (C*H*H), 3.36 (dd, $J=14.6$, 3.65) (CH*H*), 7.2–7.5 (m) (Ph)	5.05 (m), 5.38 (m)

	p-cymene					
Complex	Me	*i*Pr	AB systems	C*H	R_1	NH_2
1c[c]	2.45 (s)	1.34 (d, $J=7.0$) 1.36 (d, $J=7.0$) 2.82 (sp)	5.81, 6.12 ($J=5.8$) 5.98, 6.16 ($J=5.9$)	3.40 (m)	1.29 (d, $J=7.3$) (Me)	5.71 (pt, $J=$ 9.6), 4.91 (pt, $J=$ 9.6)
3c[c]	2.41 (s)	1.36 (d, $J=6.8$) 1.42 (d, $J=6.9$) 2.95 (sp)	5.84, 6.33 ($J=5.8$) 5.97, 6.25 ($J=5.7$)	3.40 (m)	0.94 (d, $J=7.1$) (Me) 0.99 (d, $J=6.8$) (Me) 2.32 (m) (CH)	4.69 (m), 5.70 (m)
4c[c]	2.37 (s)	1.43 (d, $J=6.8$) 1.48 (d, $J=6.8$) 3.07 (sp)	5.98, 6.02 ($J=6.1$) 6.20, 6.42 ($J=5.9$)	2.16 (m)	1.04 (s) (*t*Bu)	5.05 (dd, $J=11.2$, 7.0) 5.77 (pt, $J=$ 10.9)
5c[c]	2.42 (s)	1.32 (d, $J=6.6$) 1.34 (d, $J=6.3$) 2.85 (sp)	5.87, 6.00 ($J=5.9$) 6.10, 6.14 ($J=5.9$)	2.85 (m)	2.95 (d, $J=$ 14.1) 3.18 (dd, $J=$ 14.1, 3.6) 7.3 (m) (Ph)	4.98 (m), 5.72 (m),

Complex	C_5Me_5	NC*H	R_1R_2[d]	NR_3
6a[b]	1.82 (s)	4.38 (m)	1.10 (m), 1.6–2.1 (m) (CH_2CH_2), 3.12 (m), 3.42 (m) (CH_2N)	5.95 (m)
6b[b]	1.71 (s)	4.72 (m)	1.26 (m), 1.98 (m), 2.18 (m) (CH_2CH_2), 3.26 (m), 3.44 (m) (CH_2N)	6.64 (m)
8a[c]	1.90 (s)	3.42 (d, $J=10$)	2.0–2.3 (m) (CH_2CH_2), 3.34 (m), 4.0 (m) (CH_2N)	2.85 (s)
8b[b]	1.71 (s)	3.95 (d, $J=8.2$)	2.0–2.55 (m) (CH_2CH_2), 3.4 (m), 3.62 (m) (CH_2N)	2.90 (s)

	p-cymene					
Complex	Me	*i*Pr	AB systems	NC*H	R_1R_2[d]	NR_3
6c[c]	2.42 (s)	1.32 (d, $J=6.9$), 1.39 (d, $J=7.0$), 2.90 (sp)	5.77, 6.25 ($J=6.0$), 5.97, 6.25 ($J=6.1$)	3.32 (m)	1.65–2.15 (m) (CH_2CH_2), 3.37 (m), 4.25 (m) (CH_2N)	5.47 (m)
9c[c]	2.41 (s)	1.38 (d, $J=6.6$), 1.45 (d, $J=6.8$), 3.00 (sp)	5.86, 6.31 ($J=5.8$), 5.98, 6.27 ($J=6.0$)	3.65 (m)	1.90 -2.10 (m) (CH_2CHOH), 4.14 (dd, $J=12.0$, 5.1) (CH_2C*H*OH), 3.60 (m), 4.45 (bs) (CH_2N), 4.09 (bs) (OH)	5.53 (m)

[a] Measured at room temperature. Chemical shifts in δ from TMS as external standard. J values in hertz. Abbreviations s, singlet; bs, broad singlet; d, doublet; dd, double doublet; pt, pseudotriplet; sp, septet; m, multiplet. [b] In CD_2Cl_2. [c] In $(CD_3)_2CO$. [d] See Scheme 1. Assignment of protons given below.

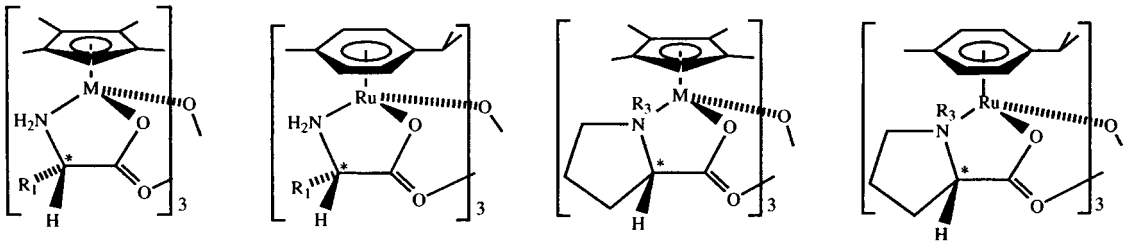

0947-6539/99/0505-1546 $ 17.50+.50/0 *Chem. Eur. J.* **1999**, *5*, No. 5

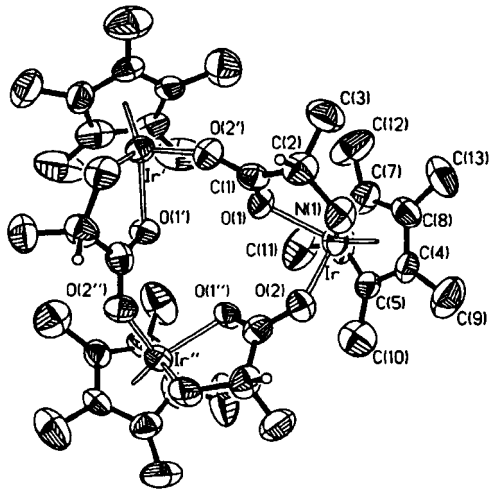

Figure 1. Molecular representation of the trinuclear cation of **1b** $[\{(\eta^5\text{-}C_5Me_5)Ir(Ala)\}_3]^{3+}$. Primed and double-primed atoms are related to the non-primed ones by the symmetry transformations $-x+y, -x+1, z$, and $-y+1, x-y+1, z$, respectively. Only the hydrogen atom on the asymmetric C(2) has been included for clarity.

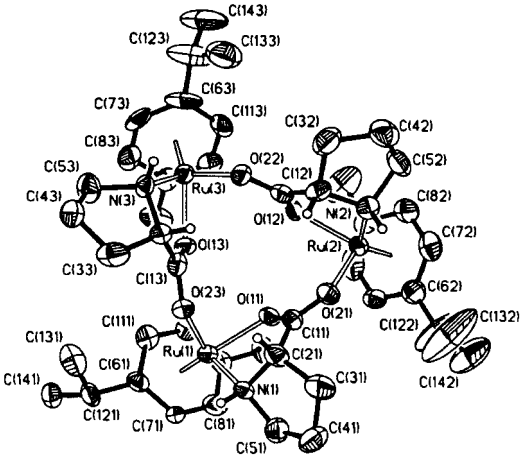

Figure 2. View of the trinuclear cation of **6c** with the atom numbering scheme. Only hydrogen atoms bonded to the two asymmetric atoms of each proline ring have been included in the drawing for clarity.

each amino acidate are bonded to a metal centre in a chelated fashion to form a five-membered metallocycle; the remaining oxygen atom coordinates to a second, different metal centre and confers an additional intermetallic bridging nature to the amino acidate ligand.

The (*N*,*O*,*O*′)-bridging tridentate coordination of α-amino acidates in transition metal complexes is rather unusual. Only two other cyclic structures have been determined previously: one is the tetramer $[(cod)RuCl(D,L\text{-}Phe)]_4$ (cod = cyclooctadiene; D,L-Phe = D,L-phenylalaninate),[11] and the second species is the trinuclear complex $[\{(\eta^5\text{-}C_5Me_5)Rh(Phe)\}_3](BF_4)_3$,[4] closely related to **1b**.

The metal coordination environments could be described as pseudo-octahedral where, in addition to the three coordination sites occupied by the amino acidate donor atoms, a π-bonded ring (pentamethylcyclopentadienyl in **1b**, or *p*-MeC_6H_4iPr in **6c**) completes the metal coordination sphere. Such coordination environments confer a chiral nature to each metal centre of both complexes. Interestingly, application of the ligand priority sequence rules to each cationic trimer[12] shows that all three metal centres in both complexes exhibit the same *R* configuration, that is for the three iridium atoms in **1b**, and for the three ruthenium atoms in **6c**.

The entire configurational characterisation of the trinuclear molecules also requires the description of the remaining chiral centres present in these molecules. The chirality of the α-carbon atom of both amino acidate ligands has been fixed in the substrate amino acid (*S*) and should not be modified under the reaction conditions. A third chiral centre appears in **6c** at the nitrogen atom of the amino acidate after coordination to the metal. According to previously determined structures,[13] and with a conformational analysis carried out for chelate prolinate complexes based on the interdependence of torsional bond angles on both five-membered fused rings (metallocycle and prolinate),[14] the chirality observed at the nitrogen atoms (*S*) is in all cases identical to that exhibited by the α-carbon of the amino acidate ligand. As a summary, we can characterise the diastereomers obtained in the solid state with the chiral descriptors $R_{Ir}R_{Ir}R_{Ir}S_CS_CS_C$ for **1b** and $R_{Ru}R_{Ru}R_{Ru}S_CS_CS_CS_NS_NS_N$ for **6c**. An identical configuration, $R_{Rh}R_{Rh}R_{Rh}S_CS_CS_C$, is present in the solid state for the closely related phenylalaninate complex $[\{(\eta^5\text{-}C_5Me_5)Rh(Phe)\}_3]^{3+}$.[4, 15]

Within the trinuclear cation **1b**, both Ir–O bonding interactions are apparently of a similar strength as reflected by the statistically identical bond lengths observed, 2.130(7) and 2.116(9) Å (Table 2). The Ir–N bond length is also in this range, 2.122(13) Å. These coordination bond lengths of the alaninate ligand compare well with the values observed in the related rhodium phenylalaninate complex $[\{(\eta^5\text{-}C_5Me_5)Rh(Phe)\}_3]^{3+}$ (mean values of 2.115(3), 2.137(3) and 2.136(4) Å, respectively). However, the Ir–O bond lengths in these bridging carboxylato complexes are slightly longer than the values observed in mononuclear $(\eta^5\text{-}C_5Me_5)Ir^{III}$ compounds where α-amino acidates are coordinated in a bidentate *N*,*O*-chelated fashion, such as in $[(\eta^5\text{-}C_5Me_5)IrCl(L\text{-}pro)]$ (Ir–O: 2.086(5) and Ir–N: 2.136(6) Å),[1] $[(\eta^5\text{-}C_5Me_5)Ir(allylglicinato)]$ (2.085(8) and 2.107(7) Å),[16] $[(\eta^5\text{-}C_5Me_5)Ir(C{\equiv}CCMe_3)(L\text{-}pro)]$ (2.105(5) and 2.135(6)Å)[17] and $[(\eta^5\text{-}C_5Me_5)IrCl(2\text{-methyl-3-dimethylaminobutanoato})]$ (2.076(9) and 2.158(11) Å),[18] probably as a consequence of

Table 2. Selected bond lengths [Å] and angles [°] for the trimeric cation of **1b**.[a]

Ir–N(1)	2.122(13)	Ir–C(7)	2.16(2)
Ir–O(1)	2.130(7)	Ir–C(8)	2.147(14)
Ir–O(2)	2.116(9)	Ir–G[b]	1.76(2)
Ir–C(4)	2.123(13)	N(1)-C(2)	1.51(2)
Ir–C(5)	2.144(14)	C(1)-O(1)	1.24(2)
Ir–C(6)	2.16(2)	C(1)-O(2′)	1.27(2)
N(1)-Ir-O(1)	78.4(6)	Ir-O(1)-C(1)	116.2(10)
N(1)-Ir-O(2)	77.8(5)	Ir-N(1)-C(2)	111.0(9)
N(1)-Ir-G[b]	134.1(7)	O(1)-C(1)-O(2′)	124.4(13)
O(1)-Ir-O(2)	86.8(4)	O(1)-C(1)-C(2)	119.9(13)
O(1)-Ir-G[b]	131.0(7)	O(2′)-C(1)-C(2)	115.8(13)
O(2)-Ir-G[b]	129.1(6)	C(1)-C(2)-C(3)	109.2(13)

[a] The symmetry transformation used to generate primed atoms is: $-x+y, -x+1, z$. [b] G represents the centroid of the coordinated pentamethylcyclopentadienyl ring.

the greater electron density withdrawing occasioned by the bridging bonding mode of the carboxylate ligand.

The bridging coordination of the L-prolinate ligand in **6c** to the isoelectronic '(η^6-*p*-MeC$_6$H$_4$*i*Pr)Ru' moiety generates bond lengths and angles around the metal analogous to those reported for **1b** (Table 3). The Ru–Aa bond lengths (av Ru–N 2.116(6), av Ru–O(1) 2.096(5), av Ru–O(2) 2.121(5) Å) are in good agreement with the average values observed in *N,O*-chelate α-amino acidato–Ru^{II} complexes (av Ru–N 2.128(9), av Ru–O 2.096(7) Å).[19] Interestingly, within experimental error, the carboxylate group acts in both complexes as a symmetrical bridging ligand.

Table 3. Selected bond lengths [Å] and angles [°] for the trimeric cation of **6c**.[a]

	(1)[a]	*(2)*[a]	*(3)*[a]
Ru–N	2.109(9)	2.109(10)	2.131(9)
Ru–O(1)	2.098(7)	2.089(7)	2.101(8)
Ru–O(2)	2.132(8)	2.121(8)	2.109(9)
Ru–C(6)	2.231(12)	2.168(14)	2.207(13)
Ru–C(7)	2.137(12)	2.147(14)	2.162(12)
Ru–C(8)	2.145(14)	2.176(13)	2.204(13)
Ru–C(9)	2.164(12)	2.175(13)	2.201(12)
Ru–C(10)	2.155(13)	2.165(13)	2.182(12)
Ru–C(11)	2.188(12)	2.181(12)	2.175(12)
Ru–G[b]	1.652(5)	1.650(6)	1.669(5)
N–C(2)	1.50(2)	1.51(2)	1.494(14)
N–C(5)	1.48(2)	1.51(2)	1.48(2)
C(1)–O(1)	1.258(14)	1.239(13)	1.275(15)
C(1)–O(2)	1.252(14)	1.267(14)	1.263(14)
N-Ru-O(1)	76.4(3)	78.3(4)	77.3(3)
N-Ru-O(2)	82.0(3)	78.4(4)	77.9(3)
N-Ru-G[b]	134.0(3)	134.8(3)	134.2(3)
O(1)-Ru-O(2)	83.1(3)	85.4(3)	85.7(3)
O(1)-Ru-G[b]	130.1(3)	129.8(3)	130.5(3)
O(2)-Ru-G[b]	131.1(3)	130.4(3)	130.9(3)
O(1)-C(1)-O(2)	123.3(10)	124.9(11)	122.1(11)
O(1)-C(1)-C(2)	119.9(10)	120.7(11)	119.9(11)
O(2)-C(1)-C(2)	116.7(10)	114.4(10)	117.9(11)

[a] Each column collects related geometrical parameters for the three analogous—but crystallographically independent—moieties '(*p*-MeC$_6$H$_4$*i*Pr)-Ru(L-pro)'. The atom labelling scheme used has been systematized adding 1, 2 or 3 to the numbering shown in this table (see Figure 1). [b] G represents the centroid of the coordinated six-membered *p*-MeC$_6$H$_4$*i*Pr rings.

Taking into account the trimeric nature of these complexes and assuming that the nitrogen atom of the prolinate compounds **6**–**9** adopt only the same configuration as the asymmetric carbon atom of the amino acidate ligand,[13, 14, 20] these compounds could exist as four diastereomers, depending on the configuration at the metal atoms: $S_MS_MS_MS_CS_CS_C$-$S_C(S_NS_NS_N)$, $S_MS_MR_MS_CS_CS_C(S_NS_NS_N)$, $S_MR_MR_MS_CS_CS_C(S_NS_NS_N)$, and $R_MR_MR_MS_CS_CS_C(S_NS_NS_N)$.[20] However, their ^{1}H NMR spectra showed only the presence of one or two of the four possible diastereomers (see below) and, interestingly, in both isomers only one set of resonances for the protons of the η-ring (the most intense ^{1}H NMR signals) appeared. Thus, the two observed isomers must have the same configuration at the three metals, that is $S_MS_MS_MS_CS_CS_C(S_NS_NS_N)$ or $R_MR_MR_M$-$S_CS_CS_C(S_NS_NS_N)$ (these are designated hereafter as σ and ρ isomers for simplification) because three sets of resonances of equal intensity would be expected for the other two isomers with different configuration at the metal centres.

Keeping in mind the different solution behaviour of the ρ and σ diastereomers (see below) we have examined the crystal structure of complex **1b** to try to obtain some information to aid understanding of this behaviour. We have considered the local supramolecular environment of a reference trimer molecule (RM)[21] by evaluating the packing potential energy (ppe) through an atom–atom interaction contribution[22] and with the inclusion of a hydrogen-bonding system. It should be stressed that the pairwise potential energy method is used only as a means to investigate *qualitatively* the different contributions of environment molecules (EM) around the reference, with no pretensions of obtaining true crystal potential energy values.[23]

The nearly spherical shape of the trimers permits pseudo hexagonal close packing. Each trimer molecule is surrounded by fourteen identical trinuclear molecules in an *ABABA* sequence (1/3/6/3/1 molecules). The detailed analysis of the relative contribution of each EM shows the six molecules in the same plane of the reference molecule (*A* layer, *ab* crystallographic plane) contribute less than 10% to the calculated ppe. Within this plane, the molecules (cation + anions) are well separated with intermolecular distances among non-hydrogen atoms longer than 7.17 Å (9.35 Å for cation–anion and 6.01 Å for anion–anion separations). This indicates that the interactions among molecules in the *ab* plane are weak and, presumably, do not exert an appreciable influence on the RM.

The most intense contributions to the ppe appear between the RM and symmetry-related molecules along the *c* axis, which belong to consecutive close-packed layers (Figure 3). Those molecules, numbered between 2 and 7 (6 and 7 not shown in Figure 3) (*B* layers), account for more than 67% of the interatomic contacts and make a significant contribution to the estimated packing energy. Interestingly, the two molecules in consecutive *A* layers (8 and 9 in Figure 3) exhibit a repulsive contribution to the ppe, which is interpreted by the presence of cation–anion ionic contributions that are not considered in the ppe calculation program.[24] In

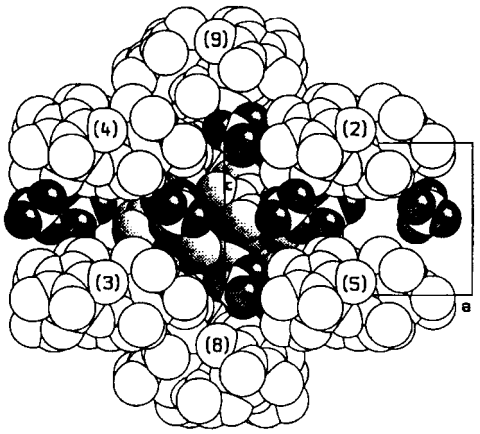

Figure 3. Space-filling model of the pseudohexagonal close-packing (*ABABA*) in **1b**; molecules in the plane of the reference molecule (RM) have been omitted for clarity. (shaded spheres: reference molecule (RM); black spheres: fluorine atoms of the BF_4 groups; open spheres: environment molecules).

0947-6539/99/0505-1548 $ 17.50+.50/0 *Chem. Eur. J.* **1999**, *5*, No. 5

fact, a search for short interatomic distances, potentially indicative of the presence of hydrogen bonding, has only revealed the existence of this type of interaction between F atoms of the BF_4 anions and aminic hydrogen atoms (Figure 4, Table 4).

Table 4. Potential hydrogen bonds[a] observed in the crystal structure of **1b**.

Atoms[b]	d(D–H) [Å]	d(D···A) [Å]	d(H···A)[Å]	∢(D–H···A) [°]
N(1)–H(1N)···F(4c) [1]	1.00(2)	2.96(4)	2.05(5)	143(2)
N(1)–H(1N)···F(1d) [1]	1.00(2)	3.20(4)	2.21(5)	169(2)
N(1)–H(1N)···F(2d) [1]	1.00(2)	3.26(5)	2.45(5)	137(2)
N(1)–H(1N)···F(3d) [1]	1.00(2)	3.26(6)	2.49(5)	133(2)
N(1)–H(1N)···F(2c) [1]	1.00(2)	3.14(4)	2.21(4)	154(2)
N(1)–H(2N)···F(2a)	0.99(2)	3.54(4)	2.56(4)	171(2)
N(1)–H(2N)···F(2b)	0.99(2)	3.09(7)	2.17(7)	155(2)
C(3)–H(3a)···F(2c) [1]	0.97(3)	3.17(5)	2.34(5)	142(2)

[a] Only distances shorter than 2.70 Å were considered (0.2 Å over the sum of Van der Waals radii). [b] All disordered BF_4 groups were included in the calculation. [c] Symmetry transformation labelled with [1] refers to $x, y, z-1$.

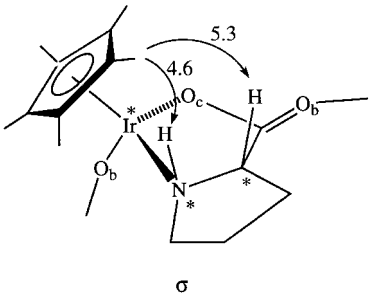

Figure 5. Selected NOE effects (%) for the iridium L-prolinate trimer **6b**, in dichloromethane. Only one monomer is shown for the sake of clarity.

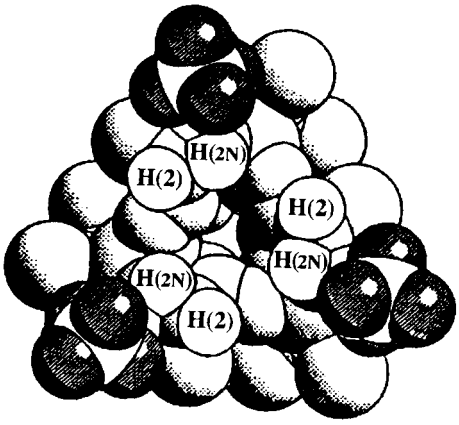

Figure 4. Space-filling model of ρ-**1b** showing the location of the aminic hydrogen atoms (H(1N) and H(2N)), which are hydrogen-bonded to the chiral C(2) carbon (H(2)). The relative location of one BF_4 group is also included. (Shaded spheres: carbon atoms; open spheres: hydrogen atoms; black spheres: fluorine atoms of the BF_4 anions).

As a whole, crystal packing in **1b** seems to be fundamentally controlled by a great number of hydrophobic (non-polar) interactions among most atoms situated on the surface of the trimer molecules and a reduced number of hydrogen bonds (polar interactions) between fluorine atoms of the BF_4 anions and the aminic hydrogen atoms. The tridentate coordination of amino acidate ligands, together with the relative low conformational freedom of the trimers, force the oxygen atoms of the carboxylate groups—potentially excellent hydrogen-bond acceptors—to be on the internal side of the molecule, which makes their participation in interatomic intermolecular interactions impossible.

Iridium and rhodium compounds: solution studies[25]

In dichloromethane or acetone: The proton NMR spectra of the iridium trimers in [D_2]dichloromethane consisted of only one set of signals, attributable to the presence of only one isomer. In this solvent, NOE difference spectra for the iridium L-prolinate complex **6b**, showed enhancement of the signal due to the NH proton (4.6%) and to the C*H proton of the amino acidate (5.3%) and no NOE effect for the CH_2 protons adjacent to the asymmetric carbon, while the C_5Me_5 protons were irradiated (Figure 5). These results support that complex **6b** exists as the σ isomer in CH_2Cl_2. Correlations of metal configuration among the series of iridium trimers can be inferred from solution chiroptical properties. The circular dichroism spectrum of compound **6b** in CH_2Cl_2 (Figure 6), consisted of two main absorption maxima, with a positive Cotton effect for the higher energy band and negative for the other. No CD transitions have been observed for the parent α-amino acid ligands above 230 nm. This suggests that the measured absorptions are mostly due to metal transitions. The CD spectra in Figure 6 (bottom) clearly indicate a pseudo-

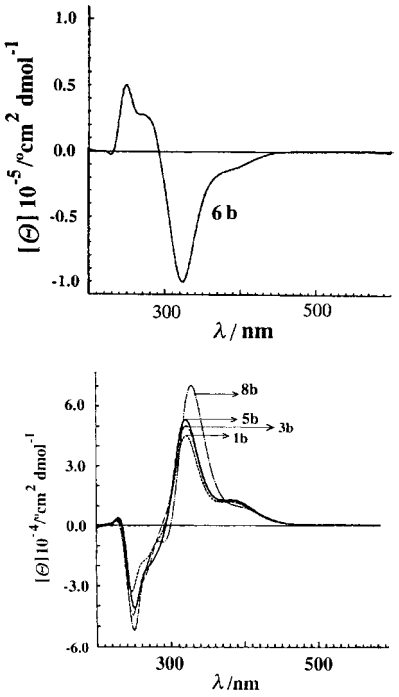

Figure 6. Circular dichroism spectra of iridium trimers in dichloromethane. Top: [{(η^5-C_5Me_5)Ir(L-Pro)}$_3$](BF_4)$_3$ (**6b**). Bottom: [{(η^5-C_5Me_5)-Ir(Ala)}$_3$](BF_4)$_3$ (**1b**), [{(η^5-C_5Me_5)Ir(Val)}$_3$](BF_4)$_3$ (**3b**), [{(η^5-C_5Me_5)-Ir(Phe)}$_3$](BF_4)$_3$ (**5b**), and [{(η^5-C_5Me_5)Ir(Me-Pro)}$_3$](BF_4)$_3$ (**8b**).

enantiomorphic relationship between the optically pure iridium trimers **1b**, **3b**, **5b**, and **8b** versus **6b**, since similar morphologies but opposite Cotton effects were observed. This observation leads to the assignment of ρ configuration to the aforementioned iridium trimers in dichloromethane solution.

The proton NMR spectra of the iridium trimers in [D_6]acetone solution consisted of only one set of signals, except for the prolinate complexes **6b** and **7b**, which showed the presence of two diastereomers in a 73/27 molar ratio.[26] NOE difference spectra for the iridium phenyl alaninate complex **5b**, showed enhancement of the signal due to the phenyl protons (4.3%) and no NOE effect for the proton bound to the asymmetric carbon atom of the amino acidate, while the C_5Me_5 protons were irradiated. These results support that the ρ isomer of complex **5b** was present in acetone solution (Figure 7). The circular dichroism spectrum

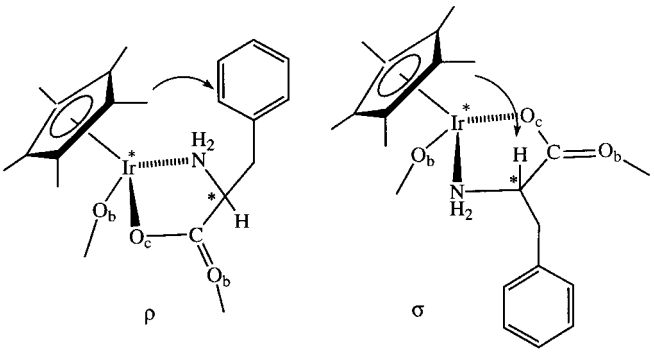

Figure 7. Selected NOE effects for the iridium phenyl alaninate trimer **5b**, in acetone. The observed interaction between the C_5Me_5 group and the C*H proton for the σ diastereomer are outlined. Only one monomer is shown for sake of clarity.

of compound **5b** in acetone (Figure 8) consisted of one main absorption maximum, with a positive Cotton effect, centred at 333 nm. The iridium trimers **1b**, **3b**, **4b**, **6b**, and **8b** showed CD spectra similar to that described for **5b** (Figure 8 bottom). On the basis of the NOE measurements for **5b** and the similarity of the CD spectra of compounds **1b**, **3b**, **4b**, **6b**, and **8b** to that of **5b**, we propose that the ρ isomer was either the only or the major diastereomer observed. Evidently, the two observed isomers for complex **7b** are the two enantiomers of those observed for **6b**, as was easily derived from NMR and CD spectra.

The configuration of all compounds remained unchanged for days, in both solvents. In particular, the diastereomer molar ratio for the L-prolinate complex **6b**, in CD_2Cl_2, remains at 73/27 for seven days at room temperature, as assayed by NMR and CD spectroscopies.

Following a similar methodology,[27] we have determined the absolute configuration for the rhodium compounds, solubility permitting.[25] In general, the behaviour is similar to that reported for the iridium ones. The only diastereomers of the rhodium trimers [{(η^5-C_5Me_5)Rh(Tle)}$_3$](BF$_4$)$_3$ (**4a**) and [{(η^5-C_5Me_5)Rh(Me-Pro)}$_3$](BF$_4$)$_3$ (**8a**) detected in dichloromethane, and of the [{(η^5-C_5Me_5)Rh(Val)}$_3$](BF$_4$)$_3$ (**3a**), [{(η^5-C_5Me_5)Rh(Tle)}$_3$](BF$_4$)$_3$ (**4a**), [{(η^5-C_5Me_5)Rh(Phe)}$_3$](BF$_4$)$_3$ (**5a**), and [{(η^5-C_5Me_5)Rh(Me-Pro)}$_3$](BF$_4$)$_3$ (**8a**) in acetone,

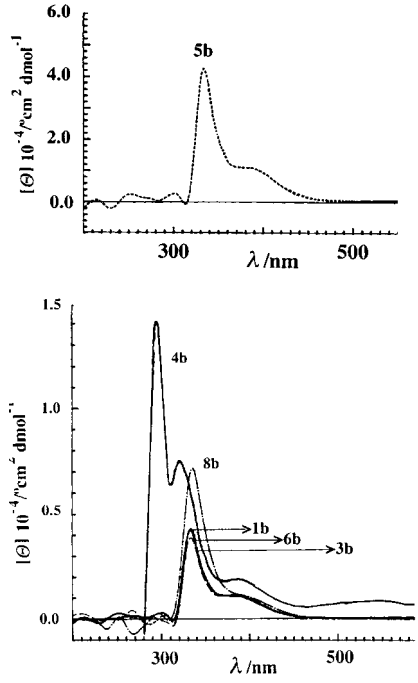

Figure 8. Circular dichroism spectra of iridium trimers in acetone. Top: [{(η^5-C_5Me_5)Ir(Phe)}$_3$](BF$_4$)$_3$ (**5b**). Bottom: [{(η^5-C_5Me_5)Ir(Ala)}$_3$](BF$_4$)$_3$ (**1b**) [{(η^5-C_5Me_5)Ir(Val)}$_3$](BF$_4$)$_3$ (**3b**), [{(η^5-C_5Me_5)Ir(Tle)}$_3$](BF$_4$)$_3$ (**4b**), [{(η^5-C_5Me_5)Ir(L-Pro)}$_3$](BF$_4$)$_3$ (**6b**), and [{(η^5-C_5Me_5)Ir(Me-Pro)}$_3$](BF$_4$)$_3$ (**8b**).

were the ρ isomers. The prolinate complex **6a** again was an exception; in dichloromethane only the σ diastereomer was observed and, in acetone, this isomer was the major component of an approximately 27/73 mixture of ρ and σ isomers. As stated for the iridium compounds, their rhodium analogues are also configurationally stable in both solvents. In particular, complexes **3a**, **5a**, **6a**, and **8a** do not isomerise in $(CD_3)_2CO$ over a period of seven days at room temperature.

In methanol: All the trimers underwent diastereomerisation processes in methanol. At room temperature, freshly prepared solutions contained mixtures of the ρ and σ isomers. The concentration of the σ diastereomer increased slowly with time and, in general, equilibrium was not reached after three hours at room temperature.[28, 29] The rate of diastereomerisation was greater for the rhodium than for the iridium trimers. In all cases, the equilibrium was reversibly shifted to the σ isomers at higher temperatures (to the ρ isomers for the prolinate complexes), as assayed by ^{1}H NMR and CD spectroscopies. As representative cases, after three hours in methanol at approximately 28 °C, the ρ/σ ratios for the iridium alaninate compound **1b** and for the phenyl alaninate analogue **5b** were 81/19 and 34/66, and the values of this ratio changed to 73/27 and 20/80, after the solutions were maintained for three additional hours at approximately 47 °C. The ratio reverted to 79/21 and 27/73 after the temperature was lowered to 28 °C.

For reasons of rate and solubility convenience, the constant for the equilibrium (a) was determined in the range 270–318 K, by integration of peaks in the ^{1}H NMR spectra of the

tbcrules=none$\check{\text{e}}$ $R_{Rh}R_{Rh}R_{Rh}S_CS_CS_C$-**4a** $\rightleftharpoons$ $S_{Rh}S_{Rh}S_{Rh}S_CS_CS_C$-**4a** (a)
ρ σ

0947-6539/99/0505-1550 $ 17.50+.50/0 *Chem. Eur. J.* **1999**, *5*, No. 5

equilibrated solutions. The equilibrium obeyed a simple van't Hoff dependence with the temperature, with $\Delta H^\circ = 23.4 \pm 0.5\ \mathrm{kJ\,mol^{-1}}$ and $\Delta S^\circ = 80.6 \pm 1.7\ \mathrm{J\,K^{-1}\,mol^{-1}}$ (Figure 9).

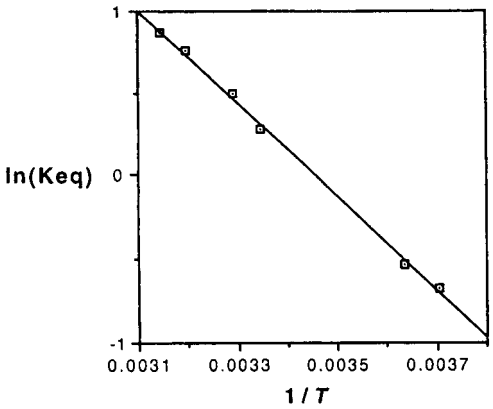

Figure 9. Van't Hoff plot for the diastereomerisation of $[\{(\eta^5\text{-}C_5Me_5)\text{-}Rh(Tle)\}_3](BF_4)_3$ (**4a**) in methanol.

On the other hand, the rate of the isomerisation of the iridium compound $[\{(\eta^5\text{-}C_5Me_5)Ir(Me\text{-}Pro)\}_3](BF_4)_3$ (**8b**) at

$$R_{Ir}R_{Ir}R_{Ir}S_CS_CS_CS_NS_NS_N\text{-}\mathbf{8b} \underset{k_{-1}}{\overset{k_1}{\rightleftharpoons}} S_{Rh}S_{Rh}S_{Rh}S_CS_CS_CS_NS_NS_N\text{-}\mathbf{8b}$$

51 °C was adequate to be monitored by ^{1}H NMR spectroscopy . Integration of the C_5Me_5 resonances assignable to the ρ and σ isomers affords the kinetic data. A first-order rate law was obtained (Figure 10)[30] with a rate constant k of $2.45 \pm 0.01 \times 10^{-5}\,\mathrm{s^{-1}}$. The value of the equilibrium constant for (b) at 51 °C,

$$\ln\{([\rho\text{-}\mathbf{8b}]_0 - [\rho\text{-}\mathbf{8b}]_e) / ([\rho\text{-}\mathbf{8b}]_t - [\rho\text{-}\mathbf{8b}]_e)\} = kt = (k_1 + k_{-1})t$$

determined by integration of the ^{1}H NMR spectra of equilibrated solutions, was 0.389.

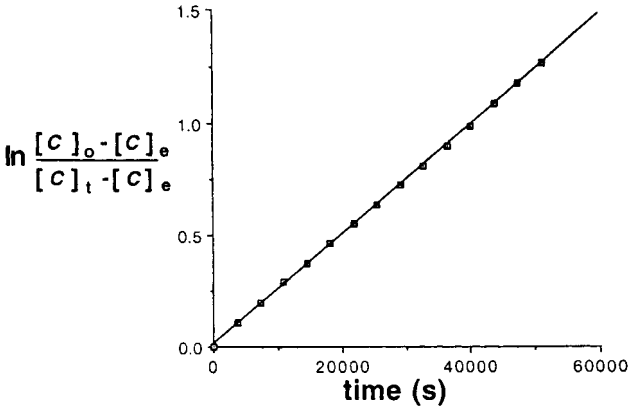

Figure 10. Kinetic plot for the diastereomerisation of $[\{(\eta^5\text{-}C_5Me_5)Ir(Me\text{-}Pro)\}_3](BF_4)_3$ (**8b**) in methanol.

In water: The ^{1}H NMR spectra of the water soluble rhodium or iridium complexes **1b**, **4a**, **4b**, **6a**, **6b**, and **8b** showed the presence of only one set of signals. The *N*-methyl-L-prolinate rhodium compound **8a** showed two sets of signals assignable to two diastereomers in a 95/5 molar ratio. In contrast to the dichloromethane or acetone solutions, the CD spectra in water were uninformative, showing no noticeable maxima in the 200–600 nm region. These experimental facts could be explained by the assumption that a rapid interconversion, on the proton NMR time scale, between the ρ and σ diastereomers took place. In order to confirm or discard this proposal, a drop of D_2O was added to a 81/19 ρ/σ diastereomeric mixture of the iridium alaninate trimer $[\{(\eta^5\text{-}C_5Me_5)\text{-}Ir(Ala)\}_3](BF_4)_3$ (**1b**) in CD_3OD, and the resulting solution was monitored by proton NMR spectroscopy. The addition produced an instantaneous partial isomerisation from the ρ to the σ diastereomer and the σ isomer was the only species present when the amount of water added was increased to approximately 15% of the total volume of the solution.[31] Analogously, it was shown that only the σ diastereomer of the complexes **4a** and **4b** was present in water. However, the unique or major diastereomer for the prolinate complexes **6a**, **6b**, **8a**, and **8b** was the ρ isomer. Complexes **8a** and **8b** underwent a slow diastereomerisation process from the ρ to the σ isomer (**8a**: from 95/5 to 79/21, six days, 22 °C; **8b**: from 100/0 to 87/13, 13 hours, 90 °C).[32] These results excluded the existence of a rapid isomerisation process and indicated that the species were rigid under these experimental conditions. With respect to the measured CD spectra, strong solvent effects on the circular dichroism transitions have been previously reported and it has been pointed out that they could arise from conformational changes and solvent interactions with the electric transition dipole moments.[33]

It is worthy of mention that from different solvents and solution compositions, the crystallised products were always the pure ρ diastereomers for both iridium and rhodium trimers (the σ isomers for the prolinate compounds). Thus, when an aqueous solution containing pure alaninate iridium trimer σ-**1b** was evaporated to dryness and the resulting yellow microcrystals were completely redissolved in dichloromethane, the ^{1}H NMR and CD spectra showed the presence of only the ρ-**1b** diastereomer. Similarly, the residue obtained when an aqueous solution of the tertleucinate rhodium complex σ-**4a** is dried, consisted of pure ρ-**4a** as shown by its ^{1}H NMR and CD spectra in acetone.

Ruthenium compounds: solution studies[25]

In dichloromethane: The X-ray single-crystal study carried out on the L-prolinate ruthenium trimer **6c** proved that the ρ isomer only was present in the crystal (see above). A sample of these single crystals was dissolved in CD_2Cl_2, and the ^{1}H NMR spectrum showed that only one diastereomer was present in solution. The corresponding CD spectrum consisted of one main absorption peak, with positive Cotton effect, centred at about 405 nm, with a shoulder shifted to higher energies. NOE difference spectra showed enhancement of the signal due to the CH_2N protons and no NOE effect for the proton bound to the asymmetric carbon atom of the amino acidate, while the aromatic protons of the *p*-MeC_6H_4iPr ligand were irradiated. These results indicated that, as in the solid, the isomer of complex **6c** observed in dichloromethane was the ρ diastereomer. In this solvent, complex ρ-**6c** isomerised slowly to σ-**6c**. The evolution, at room temperature, of the CD spectra is depicted in Figure 11.

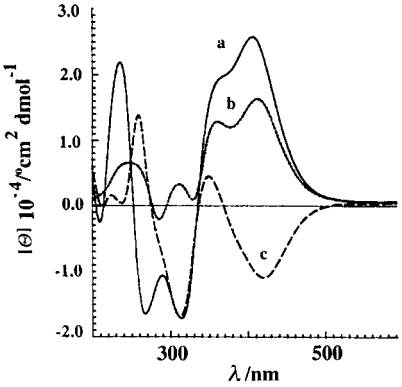

Figure 11. CD spectra of the ruthenium trimer $[\{(\eta^6\text{-}p\text{-}MeC_6H_4iPr)Ru(L\text{-}Pro)\}_3]$ $(BF_4)_3 \cdot H_2O$ (**6c**) in dichloromethane: a) immediately after dissolution, b) three and, c) seven days later.

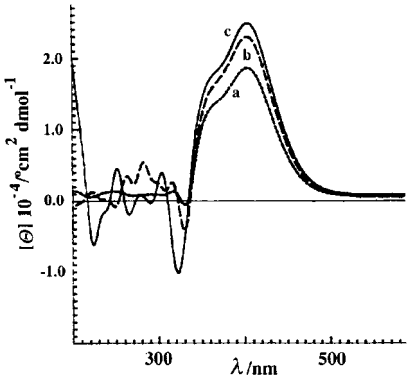

Figure 13. CD spectra of the ruthenium trimer $[\{(\eta^6\text{-}p\text{-}MeC_6H_4iPr)Ru(L\text{-}Pro)\}_3](BF_4)_3 \cdot H_2O$ (**6c**) in acetone: a) immediately after dissolution, b) six and, c) twenty days later.

Furthermore, the ^{1}H NMR spectra measured three and seven days later revealed ρ/σ ratios of 40/60 and 23/77, respectively.[26] Because this composition remained unchanged seven days later, we assume that the room temperature ρ-**6c** $\rightleftharpoons$ σ-**6c** equilibrium constant is 77/23 and the σ L-prolinate ruthenium trimer is the thermodynamically favoured isomer in this solvent. The tertleucinate and phenyl alaninate ruthenium compounds **4c** and **5c** were the only remaining ruthenium trimers soluble enough in dichloromethane to enable solution measurements.[25] In both cases, the ^{1}H NMR spectra showed the presence of only one diastereomer and, on the basis of the similarity of their CD spectra to that of the ρ-**6c** isomer (Figure 12), we assigned it ρ configuration. In contrast to the

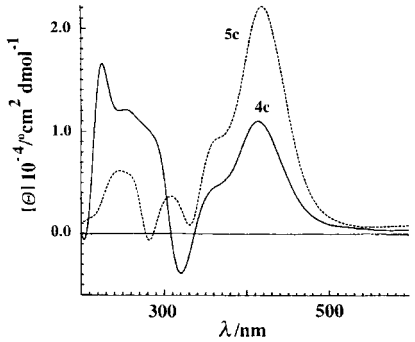

Figure 12. CD spectra of the ruthenium trimers $[\{(\eta^6\text{-}p\text{-}MeC_6H_4iPr)Ru(Tle)\}_3](BF_4)_3 \cdot H_2O$ (**4c**) and $[\{(\eta^6\text{-}p\text{-}MeC_6H_4iPr)Ru(Phe)\}_3](BF_4)_3 \cdot H_2O$ (**5c**) in dichloromethane.

solution behaviour of complex **6c**, complexes **4c** and **5c** did not diastereomerise in dichloromethane; the spectra remained unchanged after four and seven days, respectively, at room temperature.

In acetone or methanol: In these solvents, ^{1}H NMR spectra revealed the presence of only one diastereomer for the valinate (**3c**) and tertleucinate (**4c**) ruthenium compounds and mixtures of the σ and ρ isomers, enriched (> 80 %) in one of the two components, for **1c**, **5c**–**7c**, and **9c**. At room temperature, the composition of complexes **3c** and **4c** did not change with time while the others isomerised slowly to the more abundant diastereomer which then became the only species detectable by ^{1}H NMR spectroscopy after four to ten days. As a representative example, Figure 13 shows the CD spectra of the L-prolinate complex of ruthenium **6c** in acetone, immediately after dissolution, six, and twenty days later. The evolution of the spectra clearly shows the progressive increment in the optical purity of the sample. The absolute configuration of the isomers was confirmed by NOE difference spectra for an optically pure sample of the L-prolinate complex **6c** in acetone. As in dichloromethane, NOE difference spectra showed enhancement of the signal due to the CH_2N protons and no NOE effect for the proton bound to the asymmetric carbon atom of the amino acidate when the aromatic protons of the p-MeC_6H_4iPr ligand were irradiated. This result indicated that the ρ isomer of complex **6c** was the final product of isomerisation. Figure 14 clearly

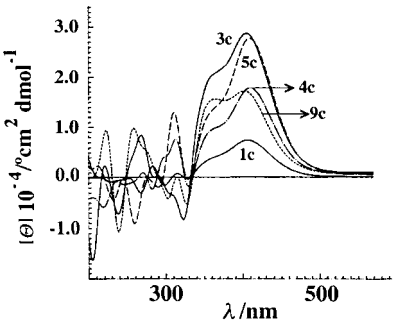

Figure 14. CD spectra of the ruthenium trimers $[\{(\eta^6\text{-}p\text{-}MeC_6H_4iPr)Ru(Ala)\}_3](BF_4)_3 \cdot H_2O$ (**1c**), $[\{(\eta^6\text{-}p\text{-}MeC_6H_4iPr)Ru(Val)\}_3](BF_4)_3 \cdot H_2O$ (**3c**), $[\{(\eta^6\text{-}p\text{-}MeC_6H_4iPr)Ru(Tle)\}_3](BF_4)_3 \cdot H_2O$ (**4c**), $[\{(\eta^6\text{-}p\text{-}MeC_6H_4iPr)Ru(Phe)\}_3](BF_4)_3 \cdot H_2O$ (**5c**), and $[\{(\eta^6\text{-}p\text{-}MeC_6H_4iPr)Ru(Hyp)\}_3](BF_4)_3 \cdot H_2O$ (**9c**) in acetone.

shows the similarity between the CD spectra of the final isomerisation products **1c**, **3c**–**5c**, and **9c** with respect to that of pure ρ-**6c**.[34] In all cases, the main feature was a maximum, with positive Cotton effect, centred at about 410 nm, with a shoulder shifted to higher energies. Consequently, we assign to all of them the ρ configuration.

In water: A crystalline sample of the L-prolinate **6c** was dissolved in D_2O and the ^{1}H NMR spectrum showed that only one diastereomer was present in solution. The corresponding CD spectrum consisted of one main absorption peak, with positive Cotton effect, centred at about 400 nm, with a

0947-6539/99/0505-1552 $ 17.50+.50/0 *Chem. Eur. J.* **1999**, *5*, No. 5

shoulder shifted to higher energies. The ρ configuration was assigned to the isomer of **6c** in aqueous solution on the basis of the X-ray crystallographic results for ρ-**6c** and the similarity of the CD spectra in the four measured solvents. Complex ρ-**6c** isomerised slowly to σ-**6c**, the ρ/σ ratio being 70/30 after seven days.[26] This ratio remained unchanged twelve days later and we assumed that the room temperature ρ-**6c** $\rightleftharpoons$ σ-**6c** equilibrium constant is 30/70. The ^{1}H NMR spectra of the ruthenium trimers **1c**, **3c**, **5c**, and **9c** consisted of two sets of resonances with 58/42, 75/25, 65/35, and 80/20 intensity ratios.[26] Their CD spectra (Figure 15) showed

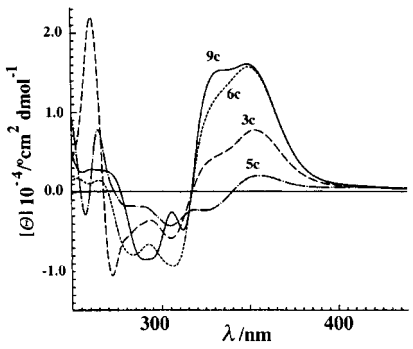

Figure 15. CD spectra of the ruthenium trimers [{(η^6-*p*-MeC_6H_4*i*Pr)-Ru(Val)}$_3$]$(BF_4)_3 \cdot H_2O$ (**3c**), [{(η^6-*p*-MeC_6H_4*i*Pr)Ru(Phe)}$_3$]$(BF_4)_3 \cdot H_2O$ (**5c**), [{(η^6-*p*-MeC_6H_4*i*Pr)Ru(L-Pro)}$_3$]$(BF_4)_3 \cdot H_2O$ (**6c**), and [{(η^6-*p*-Me-C_6H_4*i*Pr)Ru(Hyp)}$_3$]$(BF_4)_3 \cdot H_2O$ (**9c**) in water.

similar features to those of ρ-**6c** and, consequently, we assigned to the more abundant isomer the ρ configuration. Whereas compounds **1c**, **3c**, and **5c** did not isomerise, the ρ/σ ratio for the 4-OH-prolinate compound **9c** reached a constant value of 60/40 after seven days in solution.

On the other hand, a solution of pure prolinate ruthenium trimer ρ-**6c** in dichloromethane was left to isomerise to achieve a 60/40 ρ/σ ratio. During this process, a small number of yellow needles were formed. The mixture was evaporated to dryness and the residue was redissolved in CD_2Cl_2. The ^{1}H NMR spectrum exhibited a 68/32 ρ/σ ratio. In another related experiment, an aqueous solution of a 65/35 ρ/σ ratio mixture of the phenylalaninate ruthenium trimer **5c** was evaporated to dryness. The composition of the residue in CD_2Cl_2 was the same as in the aqueous solution, within experimental error. Thus, in contrast to the rhodium and iridium trimers behaviour, the solid-state composition of the ruthenium trimers depends on the composition of the solutions from which they originated. Table 5 summarises the equilibrium compositions for complexes **1**–**9** in the four solvents investigated.

Exchange processes: An equimolar mixture of the tertleucinate rhodium and iridium complexes [{(η^5-C_5Me_5)M(Tle)}$_3$]-$(BF_4)_3$ (M = Rh (**4a**), Ir (**4b**)) was dissolved in CD_3OD at $-77\,^\circ$C and monitored by ^{1}H NMR spectroscopy. An initial ^{1}H NMR spectrum was immediately recorded at $-84\,^\circ$C and it revealed that only the two starting compounds were present in the solution but, five minutes later at the same temperature, new signals emerged in the C_5Me_5 region. At room temperature, the spectrum showed nine new resonances in this region

Table 5. Equilibrium diastereomer ratio (ρ/σ)[a] for complexes **1**–**9** in different solvents

Metal	Rh	Ir	Ru
dichloromethane			
amino acidate[b]	> 98/2	> 98/2	> 98/2
L-Pro	< 2/98	< 2/98	23/77
acetone			
amino acidate[b]	> 98/2	> 98/2	> 98/2
L-Pro	27/73	73/27	> 98/2
methanol:			
amino acidate[c]	[d]	[d]	> 98/2
water:			
Tle	< 2/98	< 2/98	[e]
Ala	–	< 2/98	[e]
L-Pro	> 98/2	> 98/2	70/30
Me-Pro	[f]	[f]	–
Hyp	–	–	60/40

[a] The ratio values > 98/2 or < 2/98 are quoted when only one of the two isomers was detected, at equilibrium, by ^{1}H NMR spectroscopy. [b] All the measured amino acidates except the L-prolinate. [c] All the measured amino acidates. [d] Variable ρ/σ ratio values. The proportion of the σ isomer increases with temperature. [e] Variable ρ/σ ratio values (see text). [f] The equilibrium was not achieved.

and a FAB$^+$ mass spectrum of the solution revealed peaks at *m/z* values of 828, 1196, and 1285, assignable to [(η^5-C_5Me_5)$_2$-$RhIr(Tle)_2$]$^+$, [(η^5-C_5Me_5)$_3$$Rh_2Ir(Tle)_3$]$^+$, and [($\eta^5$-$C_5Me_5$)$_3$-$RhIr_2(Tle)_3$]$^+$ fragments, respectively.

Transfer hydrogenation of aldehydes: Most of the experiments were carried out with citral (a 64/36 mixture of geranial/neral) and *trans*-cinnamaldehyde as substrates and with [{(η^5-C_5Me_5)Rh(L-Pro)}$_3$]$(BF_4)_3$ (**6a**) and [{(η^6-*p*-MeC_6H_4*i*Pr)Ru(L-Pro)}$_3$]$(BF_4)_3$ (**6c**) as catalysts. HCOONa and 2-propanol acted as hydrogen donors, but dioxane was completely unreactive.

Catalysis by [{(η^6-p-MeC_6H_4iPr)Ru(L-Pro)}$_3$]$(BF_4)_3$ (**6c**): Sodium formate served as a good H-donor in water/toluene biphasic systems for the reduction of citral. In one hour at 100 °C, 25.6 % geraniol and 10.5 % nerol were produced (total turnover 65). However, further heating did not result in a noteworthy change of the composition of the reaction mixture and it was shown that the reaction had stopped. It was not possible to reduce the aldehydes with 2-propanol as the *sole* reducing agent. Thus, a solution of citral in 2-propanol when refluxed at 83 °C in the presence of the Ru complex did not yield any saturated product in two hours and the geranial/neral ratio also remained unchanged. Addition of solid sodium formate (2–30 times excess over Ru) to the above solution in 2-propanol triggered a *fast reaction* of citral. Typically, in one hour, 70–146 turnovers could be achieved in refluxing 2-propanol with formate:Ru ratio as low as 2:1. Consequently, this is a *formate-assisted* hydrogen transfer from 2-propanol to citral. Similar results are obtained with cinnamaldehyde. In all cases, the reaction is selective for the formation of unsaturated alcohols and in most reactions the products of C=C hydrogenation hardly amount to 1 % of the substrate. Moreover, the *cis*:*trans* composition (64:36 in citral) remained unchanged in the product even at high conversions (Scheme 2).

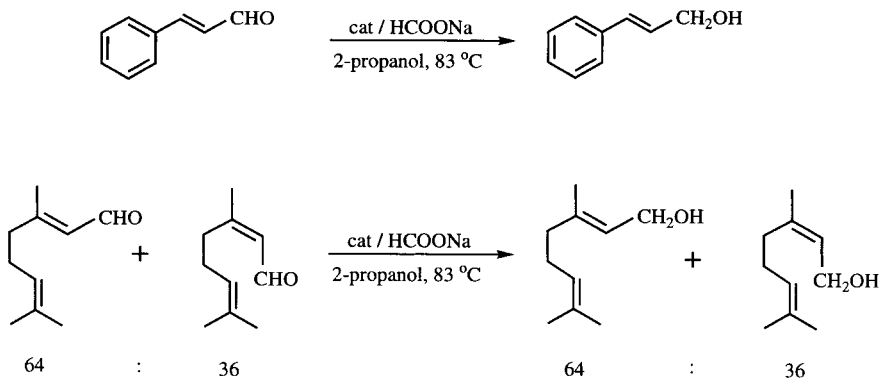

Scheme 2. Transfer hydrogenation of *trans*-cinnamaldehyde and citral with $[\{(\eta^5\text{-}C_5Me_5)Rh(\text{L-Pro})\}_3](BF_4)_3$ (**6a**) and $[\{(\eta^6\text{-}p\text{-}MeC_6H_4iPr)Ru(\text{L-Pro})\}_3](BF_4)_3$ (**6c**) as catalysts.

An intriguing unwanted feature of these catalytic reactions is that in most cases they stop at low total turnovers. Therefore, we checked several possibilities of inhibition and catalyst deactivation. In separate experiments it was established that:

i) there is no inhibition by the alcohol products,
ii) there is no inhibition by acetone,
iii) water is neither inhibitory nor advantageous for the reaction (up till 2% v/v),
iv) neat 2-propanol is much more efficient than a propanol/toluene = 1/9 mixture.

Special attention was paid to the possible effects of HCOONa. Typically, ratios of formate/ruthenium of 2, 10, and 20 were used. No striking difference could be seen in the turnovers of the various reactions due to the change in the formate concentration. Pretreatment of the Ru complex with 2 equiv of HCOONa in boiling 2-propanol prior to the addition of substrate, resulted in a solution of somewhat diminished catalytic activity (total turnover in one hour was 110 compared to the usual 146).

The reaction proved sensitive to temperature. At 58 °C, 1.46 mmol citral was reduced with 81.6% conversion in nine hours as opposed to the one hour or less reaction time at 83 °C. The reaction was preceded by an induction period of about one hour. Following the induction period, the reaction proceeded at a uniform rate until the consumption of most of the substrate.

In reduction of cinnamaldehyde, exclusive selectivity towards the formation of cinnamyl alcohol was observed both with $[\{(\eta^6\text{-}p\text{-}MeC_6H_4iPr)Ru(\text{L-Pro})\}_3](BF_4)_3$ (**6c**) and with $[\{(\eta^6\text{-}p\text{-}MeC_6H_4iPr)Ru(Phe)\}_3](BF_4)_3$ (**5c**). The latter complex proved more active (such as in acetophenone reductions, see below); conversions in one hour under standard conditions were 30.3 and 40.9%, respectively.

Catalysis by $[\{(\eta^5\text{-}C_5Me_5)Rh(\text{L-Pro})\}_3](BF_4)_3$ (**6a**). Reaction with a five times excess of HCOONa in refluxing 2-propanol gave a clear light brown solution which reduced citral to geraniol and nerol with total turnovers of 30–60 in 30–60 min. Heating the catalyst dissolved in the formate-containing 2-propanol solution for 10 min prior to the addition of the substrate led to almost complete deactivation and only seven turnovers were observed in 30 min. An interesting feature of these reactions is in that *no hydrogenation of the C=C bonds* in the substrate took place. This is in contrast to the selectivity in favour of C=C double bond reduction usually observed for Rh–phosphane catalysts.[5d]

Enantioselective transfer hydrogenation of acetophenone. *General features of the catalytic reaction:* Many of the new trimers **1**–**9** as well as the previously reported monomeric complexes $[(\eta^6\text{-}p\text{-}MeC_6H_4iPr)Ru(\text{L-Pro})Cl]$, $[(\eta^6\text{-}p\text{-}MeC_6H_4iPr)Ru(Phe)Cl]$, $[(\eta^5\text{-}C_5Me_5)Rh(\text{D-Pro})Cl]$, $[(\eta^5\text{-}C_5Me_5)Ir(\text{L-Pro})Cl]$, and $[(\eta^5\text{-}C_5Me_5)Ir(\text{Me-Pro})Cl]$ were studied as catalysts for this reaction (Scheme 3). With the exception of the *N*-methyl-prolinate complex of iridium, all the above complexes actively catalyse hydrogen transfer from 2-propanol to acetophenone (see Tables 6 and 8). The reaction

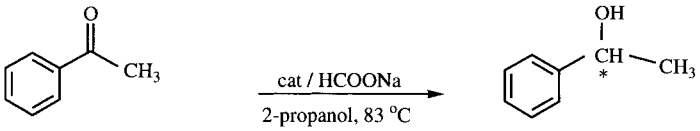

Scheme 3. Enantioselective transfer hydrogenation of acetophenone.

Table 6. Catalytic transfer hydrogenation[a] of acetophenone with 2-propanol.

Entry	Catalyst	Conv.[c] [%]	*ee*[d] [%]
1	$[\{(\eta^6\text{-}p\text{-}MeC_6H_4iPr)Ru(\text{L-Pro})\}_3](BF_4)_3$	69.9	71
2	$[\{(\eta^6\text{-}p\text{-}MeC_6H_4iPr)Ru(\text{D-Pro})\}_3](BF_4)_3$	69.3	70[e]
3	$[\{(\eta^6\text{-}p\text{-}MeC_6H_4iPr)Ru(\text{L-Pro})\}_3](BF_4)_3$[b]	67.0	71
4	$[\{(\eta^6\text{-}p\text{-}MeC_6H_4iPr)Ru(Phe)\}_3](BF_4)_3$	86.3	22
5	$[(\eta^6\text{-}p\text{-}MeC_6H_4iPr)Ru(Phe)Cl]$	87.5	23
6	$[(\eta^6\text{-}p\text{-}MeC_6H_4iPr)Ru(\text{L-Pro})Cl]$	43.3	70
7	$[\{(\eta^5\text{-}C_5Me_5)Rh(\text{L-Pro})\}_3](BF_4)_3$	8.7	60
8	$[\{(\eta^5\text{-}C_5Me_5)Rh(\text{L-Pro})\}_3](BF_4)_3$[b]	8.0	61
9	$[\{(\eta^5\text{-}C_5Me_5)Ir(\text{L-Pro})\}_3](BF_4)_3$	15.6	59
10	$[\{(\eta^5\text{-}C_5Me_5)Ir(\text{L-Pro})\}_3](BF_4)_3$[b]	20.6	64
11	$[(\eta^5\text{-}C_5Me_5)Ir(\text{L-Pro})Cl]$	17.0	58
12	$[(\eta^5\text{-}C_5Me_5)Ir(\text{Me-Pro})Cl]$	1.8	2

[a] Standard conditions, see Experimental Section. [b] 1 equiv HCOONa. [c] Conversion of acetophenone in 1 hour. [d] Enantiomeric excess of (*R*)-(+)-1-phenylethanol. [e] Enantiomeric excess of (*S*)-(−)-1-phenylethanol.

requires the addition of a base of suitable basicity. Under the standard conditions (see Experimental Section) 8 to 80% conversion of the starting material can be achieved in one hour (corresponding to 17–170 turnovers of the catalyst) to yield 1-phenylethanol with up to 75% enantiomeric excess. With L-amino acids, the major product is (*R*)-(+)-1-phenylethanol.

The fast reaction of acetophenone is preceded by an induction period. At 83 °C, with $[(\eta^6\text{-}p\text{-}MeC_6H_4iPr)Ru(\text{L-Pro})Cl]$, this lasts about 10 min but can be as long as 60 min at 61 °C (Figure 16). During the induction period, complexes of all three metals undergo characteristic changes in colour. The originally yellow solutions of the Ru complexes become red towards the end of the induction period and a tobacco

0947-6539/99/0505-1554 $ 17.50+.50/0 *Chem. Eur. J.* **1999**, *5*, No. 5

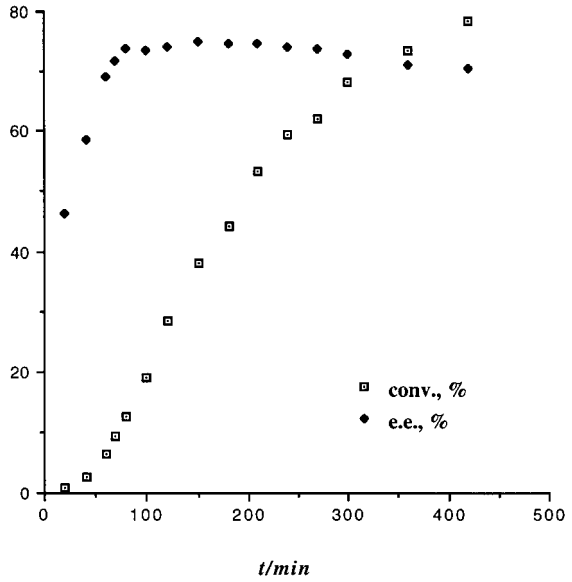

Figure 16. Conversion of the substrate and enantiomeric excess of the product (*R*)-(+)-1-phenylethanol as a function of time in transfer hydrogenation of acetophenone catalysed by [(η^6-*p*-MeC_6H_4*i*Pr)Ru(L-Pro)Cl] at 61 °C, 0.01 mmol Ru, 2.14 mmol acetophenone, 5 mL 2-propanol, 100 μL 0.2 M aqueous HCOONa.

brown colour develops at high conversion. Pale yellow Ir solutions become strong yellow and the light yellow solutions of Rh-complexes gain an orange tint during the hydrogen transfer reactions. Both the yields and enantioselectivities depend strongly on the catalyst and base used and, therefore, a systematic study of the effect of reaction variables was undertaken.

Comparison of the catalysts: The comparison of the catalysts are given in Tables 6 and 8. In general, the catalytic activity in a series with the same aminoacidate ligand varies in the order Ru > Ir > Rh. With the same metal, the use of less bulky and more flexible aminoacidate ligands generally results in increased rates with a concomitant loss in enantioselectivity. There is no substantial difference in the catalytic activity of the trimeric complexes (introduced as tetrafluoroborate salts) and the monomeric chloride compounds. Furthermore, complexes with L and D isomers of the same amino acid show the same activity and degree of enantioselectivity; with D-amino acid ligands, the expected (*S*)-(−)-1-phenylethanol is produced (Table 6, entries 1, 2).

Effect of base, chloride, or amino acid addition: It is clearly seen from the data of Table 7 that the reaction requires a *mild* base instead of KOH or NaOH, which are widely utilised to promote hydrogen transfer from 2-propanol with various catalysts. Actually, following the experimental protocol (strongly alkaline conditions, 0.01 mmol catalysts, 10 mmol acetophenone) successfully used with [$RuCl_2(PPh_3)_3$],[7b] only 1.3 % conversion was achieved in one hour which corresponds to thirteen turnovers of the [{(η^6-*p*-MeC_6H_4*i*Pr)Ru(L-Pro)}$_3$]-(BF_4)$_3$ (**6c**) catalyst.

The most suitable base additives are Na_2CO_3 and HCOONa which both promoted the reaction with equal efficiency for all

Table 7. Effect of bases on the transfer hydrogenation of acetophenone.[a]

Base	Ru[b]		Rh[c]		Ir[d]	
	conv.[e] [%]	*ee*[f] [%]	conv.[e] [%]	*ee*[f] [%]	conv.[e] [%]	*ee*[f] [%]
none	0.0	–	1.8	n. d.	5.5	55
Na_2CO_3	67.8	71	10.6	52	16.6	60
$(NH_4)_2CO_3$	1.3	37	15.7	8	4.5	n. d.
NaOH	30.8	71	8.8	40	10.3	20
HCOONa	69.9	71	8.7	60	15.6	59

[a] Standard conditions, see Experimental Section. [b] Ru = [{(η^6-*p*-MeC_6H_4*i*Pr)Ru(L-Pro)}$_3$](BF_4)$_3$. [c] Rh = [{(η^5-C_5Me_5)Rh(L-Pro)}$_3$](BF_4)$_3$. [d] Ir = [{(η^5-C_5Me_5)Ir(L-Pro)}$_3$](BF_4)$_3$. [e] Conversion of acetophenone in 1 hour. [f] Enantiomeric excess of (*R*)-(+)-1-phenylethanol.

the complexes investigated. These two bases also led to the highest enantioselectivities. Conversely, $(NH_4)_2CO_3$ was effective only in the case of [{(η^5-C_5Me_5)Rh(L-Pro)}$_3$](BF_4)$_3$ (**6a**); however, the increased activity was accompanied by a substantial decrease in enantioselectivity. NaOH gave lower but still acceptable rates with complexes of all three metals but the enantioselectivity remained high only in combination with [{(η^6-*p*-MeC_6H_4*i*Pr)Ru(L-Pro)}$_3$](BF_4)$_3$.

Taking into account its effect on the rates and selectivities in combination with all the complexes investigated, sodium formate was found to be the most suitable base and was applied in most cases. Both the rates and enantioselectivities are insensitive to small changes in the concentration of water or HCOONa (2–4 % v/v, 1 or 2 equiv of formate/metal; see, for example, Table 6, entries 3, 8, 10).

Addition of L-proline strongly inhibits catalysis by [{(η^6-*p*-MeC_6H_4*i*Pr)Ru(L-Pro)}$_3$](BF_4)$_3$; 1.6 equiv per ruthenium almost completely stop the reaction (4.2 % conversion in one hour). It is important to note, however, that the enantioselectivity (74 % *ee*) remains unaffected (see Table 2SP in Supporting Information available from the authors). Chloride has a pronounced inhibitory effect on the reaction rate (Table 6) both with [(η^6-*p*-MeC_6H_4*i*Pr)Ru(L-pro)Cl] and with [{(η^6-*p*-MeC_6H_4*i*Pr)Ru(L-Pro)}$_3$](BF_4)$_3$. With the former catalyst, at a Cl^-/Ru ratio of 15.5, hardly any reaction was observed (2.9 % conversion in one hour) and the reaction mixture remained yellow throughout; the usual colour transition to red was not apparent.

Enantioselectivity as a function of reaction time: Although the reactions of medium duration (1–3 h) showed high and reproducible enantioselection, it was observed that when larger amounts of acetophenone were subjected to reduction by hydrogen transfer over long reaction times the enantiomeric composition of the final mixture was adversely effected (see Table 1SP in Supporting Information available from the authors). However, no direct inverse relationship could be found between catalyst *turnover* and enantioselectivity and this phenomenon may be due to secondary processes which gain significance over time. It is also noteworthy that the enantioselectivity could not be increased by accelerating the reaction with more catalyst.

The change of enantioselectivity as a function of reaction time was investigated with [(η^6-*p*-MeC_6H_4*i*Pr)Ru(L-pro)Cl] at 83, 71 and 61 °C (Figure 16; see Figures 1SP and 2SP in the Supporting Information available from the authors). A

striking feature of the reaction at all temperatures is a *sharp rise* of the enantiomeric excess during the induction period. At 61 °C, the enantiomeric excess increases from 46% (20 min, 0.9% conversion) to 69% (60 min, 6.4% conversion) and this change is accompanied by the characteristic colour change of the catalyst from yellow to red. In the later phase of the reaction, the enantiomeric excess reaches a saturation value (75% at 150 min) but starts slowly decreasing at longer reaction times. This decrease is more strongly expressed at 83 °C where the *ee* falls back from its highest value, 72% at 20 min to 66% in two hours.

Pretreatment of the catalysts: Since it was known that, in most cases, the catalyst complexes change their configuration around the metal ion as a function of solvent, temperature and time (see solution studies), experiments were carried out in which the catalysts were pretreated for 30 min in aqueous 2-propanol (16.7% v/v H_2O) at 83 °C in the absence of both acetophenone and base.

In the majority of cases, this pretreatment moderately decreased the activity of the catalyst accompanied by no or only a slight change (mostly increase) in enantioselectivity (Table 8). However, the activities of both $[\{(\eta^6\text{-}p\text{-}MeC_6H_4iPr)Ru(L\text{-}Pro)\}_3](BF_4)_3$ and $[\{(\eta^6\text{-}p\text{-}MeC_6H_4iPr)Ru(Ala)\}_3](BF_4)_3$ were strongly affected (conversion of 22.9% instead of 67.0, and 25.4% instead of 86.6%), while the enantiomeric excess changed only moderately (71% instead of 70%, and 14% instead of 7%). Similar to solutions with added chloride, the pretreated Ru catalysts did not show the characteristic yellow to red colour change during the hydrogen transfer reactions.

Table 8. Effect of the pretreatment of the catalyst[a,b] on the rate and the enantioselectivity of catalytic hydrogen transfer from 2-propanol to acetophenone.

Entry	Catalyst	No pretreatment		Pretreated	
		conv.[c] [%]	*ee*[d] [%]	conv.[c] [%]	*ee*[d] [%]
13	$[(\eta^6\text{-}p\text{-}MeC_6H_4iPr)Ru(Ala)]_3(BF_4)_3$	86.6	7	25.4	14
14	$[(\eta^6\text{-}p\text{-}MeC_6H_4iPr)Ru(L\text{-}Pro)]_3(BF_4)_3$	67.0	71	22.9	70
15	$[(\eta^5\text{-}C_5Me_5)Ir(L\text{-}Pro)]_3(BF_4)_3$	20.6	64	16.7	60
16	$[(\eta^5\text{-}C_5Me_5)Ir(Tle)]_3(BF_4)_3$	33.5	43	15.3	42
17	$[(\eta^5\text{-}C_5Me_5)Ir(Ala)]_3(BF_4)_3$	57.5	15	35.3	19
18	$[(\eta^5\text{-}C_5Me_5)Rh(L\text{-}Pro)]_3(BF_4)_3$	8.0	61	15.5	66
19	$[(\eta^5\text{-}C_5Me_5)Rh(Tle)]_3(BF_4)_3$	35.1	16	28.0	29

[a] Standard conditions, with 1 equiv HCOONa, see Experimental. [b] Pretreatment as described in the text. [c] Conversion of acetophenone in 1 hour. [d] Enantiomeric excess of (*R*)-(+)-1-phenylethanol.

Enantiomerically pure (*R*)-(+)-1-phenylethanol under hydrogen transfer conditions with $[\{(\eta^6\text{-}p\text{-}MeC_6H_4iPr)Ru(L\text{-}Pro)\}_3](BF_4)_3$ catalyst did not show dehydrogenation or racemisation. Similarly, addition of 1–5 equiv of (*R*)-(+)-1-phenylethanol (per ruthenium) did not modify the enantioselectivity of acetophenone reduction.

Heterogenisation of the catalysts: Since it was conceivable that less coordination flexibility or decreased rotational freedom of the ligands attached to the metal ion may lead to an increase in enantioselectivity of the catalysts, $[\{(\eta^6\text{-}p\text{-}MeC_6H_4iPr)Ru(L\text{-}Pro)\}_3](BF_4)_3$, $[\{(\eta^6\text{-}p\text{-}MeC_6H_4iPr)Ru(D\text{-}Pro)\}_3](BF_4)_3$, $[\{(\eta^6\text{-}p\text{-}MeC_6H_4iPr)Ru(Ala)\}_3](BF_4)_3$, $[\{(\eta^5\text{-}C_5Me_5)Rh(Tle)\}_3](BF_4)_3$, and $[\{(\eta^5\text{-}C_5Me_5)Ir(Tle)\}_3](BF_4)_3$ were incorporated into sol gel glasses[35] prepared by hydrolysis of tetramethoxysilane and condensation of the resulting silanols in the presence of the said compounds. The finely ground glasses were used as solid catalysts under otherwise identical conditions as described in the Experimental Section for the soluble complexes. In general, they showed lower activities as expected and the optical yields were also markedly lower in comparison to the homogeneous systems. As an example, glass-encapsulated $[\{(\eta^6\text{-}p\text{-}MeC_6H_4iPr)Ru(D\text{-}Pro)\}_3](BF_4)_3$ yielded (*S*)-(−)-1-phenylethanol with 17.7% conversion (2 h) and 38% *ee* compared to 69.3% conversion (1 h) and 70% *ee* in a homogeneous system.

Other observations: Dioxane proved completely unsuitable as hydrogen donor for acetophenone reduction with these catalysts. As an example, $[\{(\eta^6\text{-}p\text{-}MeC_6H_4iPr)Ru(L\text{-}Pro)\}_3](BF_4)_3$ did not undergo a colour change and did not catalyse the reaction, either in presence or absence of HCOONa. Other ketone substrates such as pulegone and carvone were subjected to the same reaction conditions as acetophenone. No reaction was detected in any of these experiments. $[(\eta^6\text{-}p\text{-}MeC_6H_4iPr)Ru(L\text{-}pro)Cl]$ and $[\{(\eta^6\text{-}p\text{-}MeC_6H_4iPr)Ru(Ala)\}_3](BF_4)_3$ (the latter showed the highest activity in hydrogen transfer) were tested as catalysts of acetophenone hydrogenation with molecular H_2. Depending on the solvent, temperature and reaction time, 1.4% – 2.8% conversions were observed with enantioselectivities in the 52% – 66% range at 1 bar total pressure.

Discussion

Synthesis, characterisation, and solution studies: A general reaction for α-amino acidate rhodium, iridium or ruthenium chloride complexes of the formula $[(\eta\text{-ring})M(Aa)Cl]$ is the trimerisation of the derived cationic fragment by abstraction of the chloride by a halogen scavenger such as silver tetrafluoroborate. Following this synthetic method, a series of trimers with a family of α-amino acidate as chiral auxiliary ligand of general formula $[\{(\eta\text{-ring})M(Aa)\}_3](BF_4)_3$ was prepared for the three metals. Interestingly, only the two diastereomers with the same absolute configuration for the three metals were detected: the $R_MR_MR_M$, ρ diastereomer, or the $S_MS_MS_M$, σ diastereomer. Thus, the cyclisation process to form these trinuclear complexes occurs with chiral self-recognition among the mononuclear metal fragments. In general, in solvents of low polarity, such as dichloromethane or acetone, the ρ isomer is the thermodynamically preferred product. For the ruthenium compounds, this isomer is also preferred in more polar solvents such as methanol or water. Thus, in methanol, it was the only isomer observed by ^1H NMR spectroscopy and, in water, the equilibrium diastereomer ratio ρ/σ was always greater than one. For the rhodium

0947-6539/99/0505-1556 $ 17.50+.50/0 *Chem. Eur. J.* **1999**, *5*, No. 5

and iridium trimers in methanol, depending on the amino acidate, the ρ or the σ diastereomer was the thermodynamically preferred product; the σ isomer was favoured at higher temperatures. In water, the σ isomer was the only isomer detected by ^{1}H NMR spectroscopy at equilibrium. The prolinate derivatives behaved differently. Thus, for example, in dichloromethane, the σ isomer is more stable than the ρ isomer for all three metals, and only the ρ isomers of the rhodium and iridium prolinate trimers were detected in water. At a fixed temperature, the rates of diastereomerisation were strongly metal-dependent, increasing in the sequence Ru $\ll$ Ir $<$ Rh.

The structural analysis carried out at a supramolecular level for **1b** gave us a reasonable justification for the different stability of ρ and σ diastereomers in solution. Thus, the low number and the relatively restrained localisation of the polar groups (aminic hydrogen atoms) on the molecular surface of ρ diastereomers (Figure 4) could sterically constrain the accessibility of solvent molecules to this area reducing, consequently, the number of polar trimer solvent intermolecular interactions formed. On the other hand, for the σ diastereomer, the change of metal configuration is also associated with a change in the localisation of aminic hydrogen atoms on the surface of the molecule. Figure 17 shows a molecular

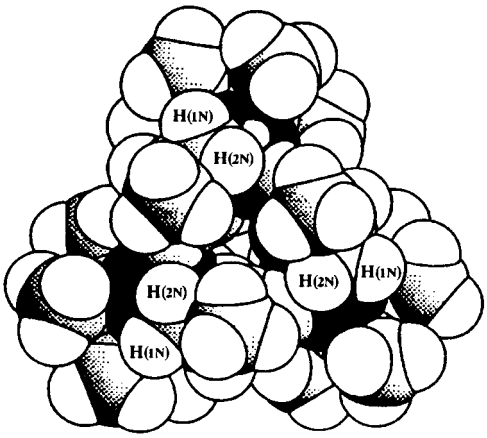

Figure 17. Molecular model of the $R_{Ir}R_{Ir}R_{Ir}R_CR_CR_C$ diastereomer (enantiomer of σ-**1b**). Hydrogen atoms of the aminic nitrogen atoms are labelled as H(1N) and H(2N). (Shaded spheres: carbon atoms; open spheres: hydrogen atoms).

model of a $R_{Ir}R_{Ir}R_{Ir}R_CR_CR_C$ trinuclear complex built up from the molecular structure of **1b** after changing the configuration at the chiral C(2) atom. This model is an enantiomeric form of the $S_{Ir}S_{Ir}S_{Ir}S_CS_CS_C$ trimer and could be considered to establish geometric arguments for σ-**1b**. The most important feature, in the context of diastereomer stability, concerns the position of polar aminic hydrogen atoms; thus in σ-**1b** diastereomer, the aminic hydrogen atoms are spread out on the molecular surface which allows interaction with solvent molecules when dissolved, with no apparent steric constrain.

This major accessibility of the polar groups in the σ-diastereomer compared to that of the ρ isomer seems to be responsible of the greater stability of the σ diastereomer in solution with increasing solvent polarity (see Table 5).

The results of the exchange reaction, along with the thermodynamic and kinetic data reported above, strongly supported a dissociative mechanism for the diastereomerisation of the ρ into the σ isomers or vice versa. The cleavage of the bridging M–O bonds of the trimers afforded mononuclear intermediates of formula $[(\eta\text{-ring})M(Aa)]^+$. These intermediates could retain or invert their configuration but, in any case, they trimerise with chiral self-recognition leading only to homochiral-at-metal complexes; trimeric species with the same configuration at the three metal atoms.

In a polar solvent, such as water, the diastereomerisations occur at higher rates, most probably due to the good solvating properties of water which stabilises the proposed monomeric intermediate.

It is also interesting to note that the ^{1}H NMR and CD spectra for all rhodium and iridium compounds revealed the same solid composition and optical purity, regardless of crystallisation solvent or composition of the solution from which the solids were isolated. All these compounds have been prepared in methanol and, in this solvent, showed variable compositions but always included both diastereomers. However, the isolated solids, in CH_2Cl_2, showed only the presence of the ρ isomer (the σ isomer in the case of the L-prolinate ligand). Consequently, crystallisation of these trimers implies an asymmetric transformation of the second kind,[36] scarcely documented for organometallic compounds.[37] Nevertheless, the composition of the ruthenium compounds depends on the pretreatment of the solution. It is possible to prepare solid ruthenium trimers of different diastereomeric composition and, eventually, separate one diastereomer, by adequate choice of the composition of the solution and/or crystallisation solvent.

The actual nature of compounds **1**–**9**, in the solid state and in solution, deserves some further comments. From the X-ray diffraction and IR measurements, as well as the conductivity and FAB$^+$ mass spectrometry data, it seems clear that all the compounds crystallise as trimers. Furthermore, the trimeric nature persists in all cases in low polarity solvents such as dichloromethane or acetone. The reported results for the rhodium or iridium species in methanol or water also support a trimeric formulation in these two, more polar, solvents. However, the reversibility of chloride dissociation from the mononuclear ruthenium compounds $[(\eta^6\text{-}p\text{-}MeC_6H_4iPr)\text{-}Ru(Aa)Cl]$ in the presence of LiCl in water, along with the values of the B coefficient in the Onsager equation, point to the presence of solvated monomers of the formula $[(\eta^6\text{-}p\text{-}MeC_6H_4iPr)Ru(Aa)S]^+$. We suggest that for the ruthenium complexes in water and probably in methanol, an equilibrium, rapid on the NMR time scale, between the monomers and trimers, with equal configurated metals, could operate ([Eq. (2) and (3)]).

$$3\,(R_{Ru},S_C)[(\eta^6\text{-}p\text{-}MeC_6H_4iPr)Ru(Aa)S]^+ \rightleftharpoons \rho\text{-}[\{(\eta^6\text{-}p\text{-}MeC_6H_4iPr)Ru(Aa)\}_3]^{3+} \quad (2)$$

$$3\,(S_{Ru},S_C)[(\eta^6\text{-}p\text{-}MeC_6H_4iPr)Ru(Aa)S]^+ \rightleftharpoons \sigma\text{-}[\{(\eta^6\text{-}p\text{-}MeC_6H_4iPr)Ru(Aa)\}_3]^{3+} \quad (3)$$

However, interconversion between R_{Ru} and S_{Ru} solvated mononuclear species should be slow on the NMR time scale in order to account for the NMR observations. Support for this

proposal stems from the relatively slow rates of epimerisation observed for the ruthenium compounds, as well as from the isolation of trimers with different ρ/σ ratio from solutions of different composition.

Catalytic properties

Hydrogenation of unsaturated aldehydes: Hydrogenation of an unsaturated aldehyde or ketone exclusively at the oxo group is an important reaction, but in most catalytic systems the reverse selectivity is observed. It has been described[38] that $[RuCl_2(PPh_3)_3]$ in combination with ethylendiamine and KOH serves as a generally applicable, highly active and chemoselective catalyst for carbonyl reduction in the presence of olefinic or acetylenic moieties. The water-soluble analogues of this ruthenium complex, $[RuCl_2(tppms)_2]$ (tppms = (3-sulfophenyl) diphenylphosphane sodium salt) and $[RuCl_2(pta)_4]$ (pta = 1,3,5-triaza-7-phosphaadanantane), were shown previously to reduce α,β-unsaturated aldehydes to the corresponding alcohols with high activity and complete selectivity, either with aqueous sodium formate[39] or with H_2[40] as reductant. Importantly, $[RhCl(tppms)_3]$ also showed high activity but preferential reduction of the *olefinic* double bond was observed.[39, 40]

In our case, with a toluene/aqueous sodium formate biphasic system, $[\{(\eta^6\text{-}p\text{-}MeC_6H_4iPr)Ru(L\text{-}Pro)\}_3](BF_4)_3$ actively catalysed the reduction of citral, while $[\{(\eta^5\text{-}C_5Me_5)Rh(L\text{-}Pro)\}_3](BF_4)_3$ decomposed under such conditions. A genuine formate-assisted hydrogen transfer from 2-propanol could be initiated by addition of HCOONa to solutions of both complexes in this solvent at reflux temperature. The reaction can also be triggered by the addition of small amounts of K_2CO_3 and NaOH, which demonstrates that in the HCOONa/2-propanol system, formate serves as a base rather than a reductant. Since, in general, hydrogen transfer from 2-propanol requires substantial amounts of strong base (usually KOH)[7] this modification allows transfer hydrogenation in nearly neutral media. Indeed, no side reactions of citral were observed in HCOONa/2-propanol in contrast to the fast non-metal-catalysed condensation reactions in KOH/2-propanol. It is again emphasised that the isomeric ratio of *cis*- and *trans*-olefins remained the same in the product alcohol as in the substrate aldehyde mixture.

Another noteworthy feature is that in the hydrogen transfer from 2-propanol to citral, catalysed by $[\{(\eta^5\text{-}C_5Me_5)Rh(L\text{-}Pro)\}_3](BF_4)_3$ *exclusive* formation of unsaturated alcohols resulted. This is a rather unusual selectivity among the reactions catalysed by rhodium complexes.[5d, 6a, 39, 40]

The possible mechanism of aldehyde reductions both with 2-propanol and with aqueous HCOONa can be incorporated into the general reaction mechanism (see below). In the case of aqueous HCOONa as hydrogen donor, the apparent hydride intermediate is generated by coordination and decomposition of $HCOO^-$ (not shown on the scheme) as demonstrated earlier.[39b] Exclusive carbonyl reduction both with the Ru- and the Rh-based catalyst can be rationalised by the preferential coordination of carbonyl oxygen to the rather hard Ru^{II} and Rh^{III} metal ions. Indeed, weak olefin coordination is indicated by the results of isomerisation reactions: allylic alcohols did not undergo redox isomerisation and allylbenzene was isomerised only very slowly with the same catalytic system ($[\{(\eta^6\text{-}p\text{-}MeC_6H_4iPr)Ru(L\text{-}Pro)\}_3](BF_4)_3$, 2-propanol, 2 equiv of HCOONa; 17 turnovers in 4.5 h) that gave good rates for reduction of citral. This is also in accordance with the unmodified *cis/trans* isomer ratio observed in the reduction of citral. The role of HCOONa in the formate-assisted hydrogen transfer is discussed in connection with transfer hydrogenation of acetophenone.

Transfer hydrogenation of acetophenone: Hydrogenation of ketones and aldehydes by hydrogen transfer from 2-propanol is one of the most widely studied reactions.[6, 7, 41] Furthermore, enantioselective reduction of prochiral ketones and imines is of fundamental importance in synthetic organic chemistry.[7, 41–43] There are several active systems for such transformations, including the recently disclosed systems which use ruthenium(II) complexes with *P,N,O*-terdentate ligands (no enantioselectivity)[44] and the Ru^{II}–phosphane/chiral diamine/KOH catalyst system[43] which gave 99% enantioselectivity in the reduction of most aromatic ketones investigated. To date only a few neutral catalytic systems of high activity and selectivity are known.[6b, 41] However, in general, the highest optical yields of acetophenone reduction with 2-propanol, catalysed by Rh–, Ru– and Ir–phosphane or chelating diamine catalysts are in the range of 70–80%.[41]

The results presented above show that a highly enantioselective reduction of acetophenone can be achieved via hydrogen transfer from 2-propanol catalysed by $[(\eta\text{-ring})M(aminoacidate)Cl]$ and $[\{(\eta\text{-ring})M(aminoacidate)\}_3](BF_4)_3$ complexes (M = Ru, Rh, and Ir). These are the first hydrogen transfer reactions catalysed by this type of chiral metal compound and, in fact, the rates and enantioselectivities compare favourably with those reported with metal phosphane or amine complexes.[7, 41]

There are several features which should be taken into consideration when devising a possible scheme for the reaction mechanism:

i) The reaction requires a *mild base* but is adversely affected by strong ones.
ii) There is no substantial difference in the catalytic properties of the monomeric and trimeric complexes.
iii) The reaction is strongly inhibited by excess amino acid and chloride.
iv) Both the rate and the *extent* of enantioselectivity depend largely on the amino acidate ligand, for all three metal ions; the bigger the steric bulk of the aminoacidate ligand the slower the reaction and the higher the enantioselectivity.
v) The reaction is preceded by an induction period during which the enantiomeric excess *increases* sharply.
vi) At long reaction times (with the corresponding larger conversions) the enantiomeric excess slightly *decreases* despite the further increase in conversion.

A tentative suggestion for a reaction mechanism which would lead to the above experimental findings is as follows: (Schemes 4 and 5). Chloride dissociation from the monomers (**I**) or solvolysis of the trimers (**II**) leads to formation of monomeric cationic complexes (**III**) with one easily accessible coordination site. This process was independently studied and

0947-6539/99/0505-1558 $ 17.50+.50/0 *Chem. Eur. J.* **1999**, *5*, No. 5

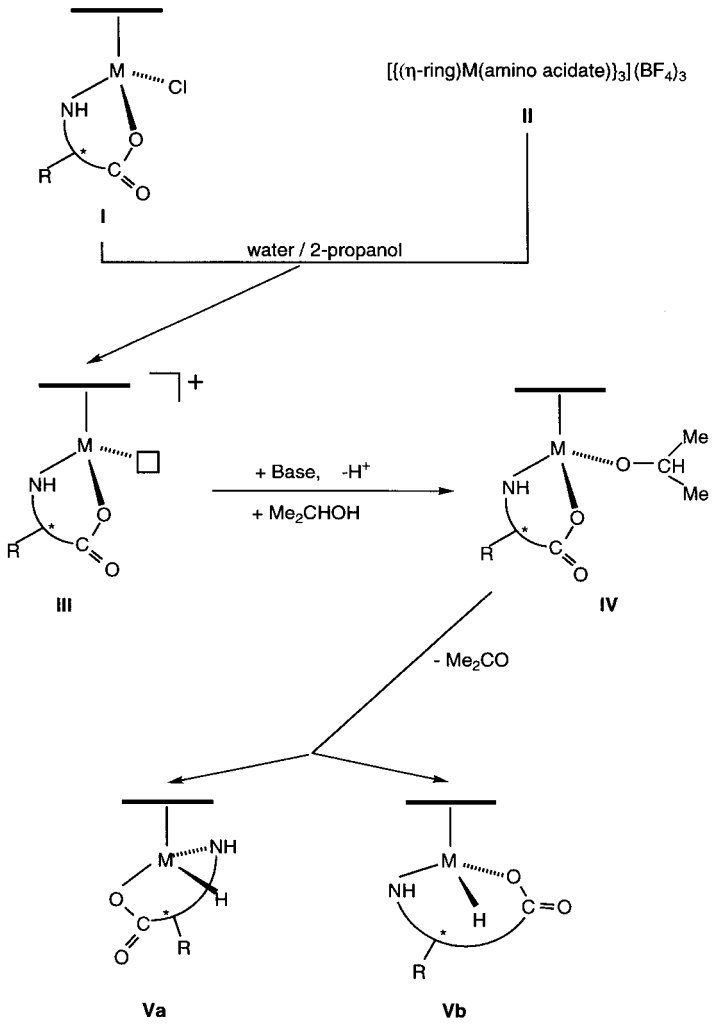

Scheme 4. Formation of chiral metal hydrides.

is strongly evidenced in the solution studies section. Base-assisted coordination of a 2-propoxy ligand gives a neutral metal compound (**IV**) with release of a proton. The latter is picked up by the base. In principle, the carboxylate ligand could serve as an internal proton acceptor. However, it does not seem basic enough to assist the deprotonation/coordination of 2-propanol, albeit there is some slow reaction with Rh and Ir complexes but not with the Ru-containing complexes in the absence of any base. Strong bases such as NaOH or KOH may lead to the formation of stable hydroxo-complexes of the $[\{(\eta\text{-ring})M\}_2(\mu\text{-}OH)_3]^+$ type,[45] which would supposedly be less or not active in catalysis because of the lack of available coordination sites.

At first glance, β-H abstraction from the 2-propoxy ligand could proceed through two distinct pathways. The required coordination site for the hydride ligand can freed either by opening the chelate ring through transient protonation of the carboxylate donor group or, perhaps more likely, by expansion of the coordination sphere. The latter implies an unusual twenty electron species that has been previously proposed for related pentamethylcyclopentadienyl rhodium derivatives.[46] By dissociation of acetone (and concomitant recoordination of the carboxylate in the case of the opening chelate ring mechanism) the coordinatively saturated monohydrides, **Va** and **Vb** can be formed.

Independent of the actual sequence of the molecular steps, the final solution may contain both the (*R*) and (*S*) epimers (with relation to metal configuration) of the supposed monohydrido-metal complex since epimerisation can take place in all the complexes **II**–**V**. The steric bulk of the aminoacidate ligand may restrict such stereochemical reorganisation. Unfortunately, only the epimerisation of the starting metal complexes could be studied independently (see solution studies) and those data are not applicable to the case of the supposed hydride complexes under different conditions. Assuming no change in the configuration of the N and C stereocentres of the amino acidate ligand, the high enantioselectivity seems to indicate that, under our experimental conditions, *formation of **Va** or **Vb** is highly diastereoselective*.

Thus, hydrides **V** would be the real catalysts (Scheme 5). Hydrogen transfer from isopropyl alcohol to acetophenone by hydrido complexes usually implies the initial formation of a 1-phenylethoxy intermediate (**VIIa**) followed by exchange of alkoxy groups (**VIIa** → **IV**).[6, 7, 41] The formation of **VIIa** from **VIa**, a critical step to account for the observed enantioselectivity, deserves some comment. Either η^1- or η^2-coordination of acetophenone requires a free coordination site on the metal ion, which again can be made available by expansion of the coordination sphere or by the opening of the amino acidate chelate ring. Assuming η^1 coordination, the intermediate should be **VIa**, which could explain the formation of (*R*)-(+)-1-phenylethanol as the major product of the acetophenone reduction. In this context, steric repulsion between the phenyl ring of acetophenone and the large C_5Me_5 (η^6-*p*-MeC_6H_4*i*Pr) and/or the amino acidate ligand leads to the highly selective production of (*R*)-(+)-1-phenylethanol in subsequent steps of the catalytic cycle (e.g. **VIa** → **VIIa** → **IV**).

Another attractive possibility is that the hydrogen transfer occurs through a six-membered cyclic structure, as shown in **VIa′**, recently proposed by Noyori et al.[6b, 47] Consistent with this view, in which the NH linkage can stabilise the transition state by the formation of a hydrogen bond, practically no reaction was observed with the *N*-methylprolinatoiridium complex (entry 12, Table 6). The possible participation of intermediates **VIa** or **VIa′** could be modulated by the nature of the hydrido ligand and is strongly influenced by the type of metal. Further work in this subject is needed.

It is remarkable that, in spite of these diverse possibilities of coordination, a high degree of enantioselectivity is observed in the transfer hydrogenation of acetophenone. The suggested catalytic cycle is in accord with most of the findings mentioned earlier:

i) A base is required to assist the heterolytic activation of 2-propanol but in order to avoid formation of stable hydroxo complexes, a *mild* base is preferred; moreover, if decoordination/recoordination of the carboxylate ligand is important, the system cannot be strongly basic.
ii) Monomeric and trimeric complexes give the same solvolysed species (**III**) and therefore show the same catalytic properties.
iii) Added chloride shifts the **I** ⇌ **III** equilibrium in favour of **I** for the most active ruthenium species and excess amino

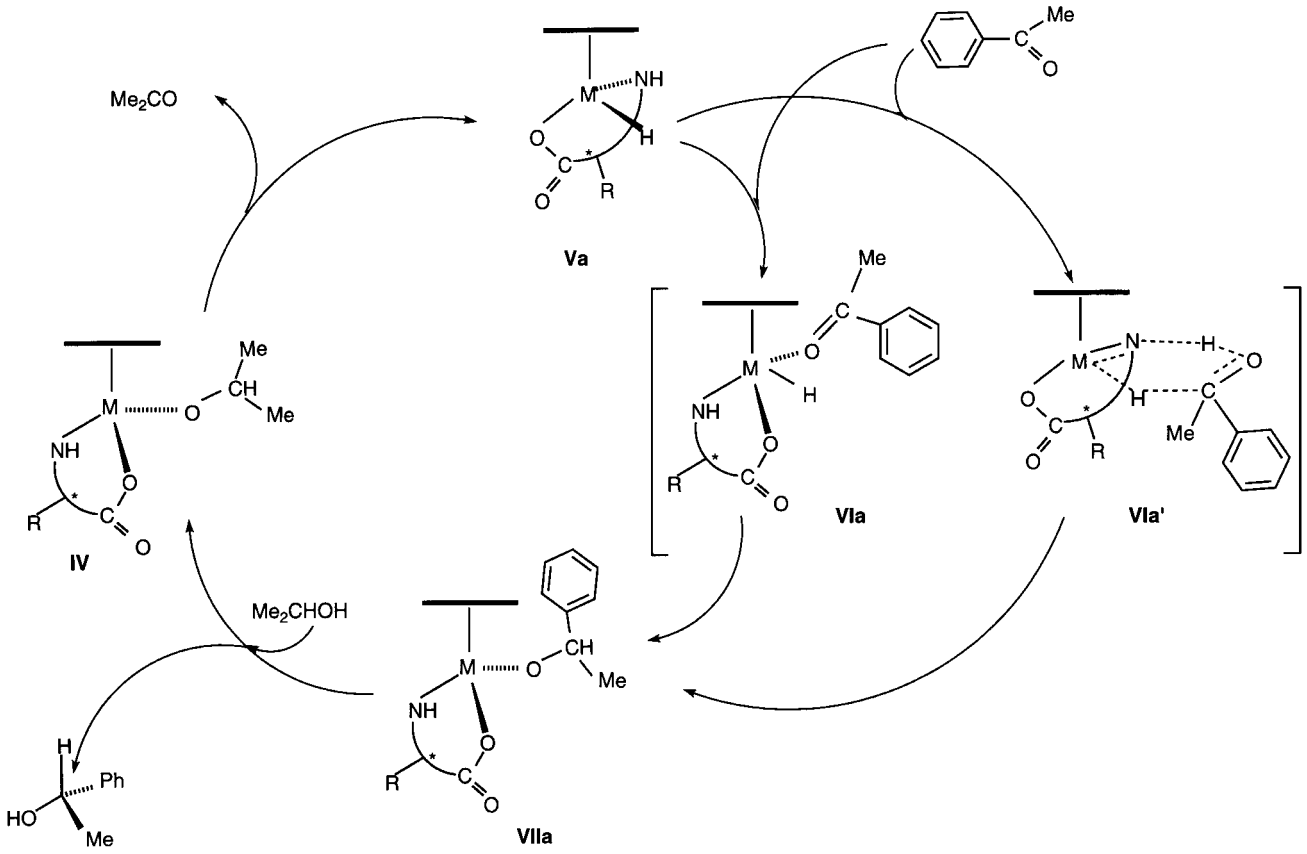

Scheme 5. Proposed catalytic cycles.

acid may be strongly coordinated, most probably also in **III**.

iv) The steric bulk of the amino acidate ligand is important in that it restricts the coordination of acetophenone to one (a few) of the possible geometries, leading to lower catalytic activity but higher enantioselectivity.

v) Replacement of L-amino acidate ligands with the respective D-enantiomers results in the formation of enantiomeric metal complexes with the same reactivity; these catalyse the formation of (*S*)-(−)-1-phenylethanol with the same activity and enantioselectivity.

An intriguing feature of the reaction is the sharp rise of enantioselectivity in the first period of the reaction. The pretreatment experiments (Table 8) were undertaken with the aim of establishing any stereochemical equilibria in advance which would be established anyway during this time. Based on the results of the solution studies, it was anticipated that a pretreatment and running the reaction in 16,67% aqueous 2-propanol could strongly influence the stereochemical outcome of the catalytic reaction compared to the selectivity obtained under standard reaction conditions (1.87% water, v/v). However, the enantiomeric excesses *did not change* significantly with one exception where the rate was considerably decreased. These results show that the catalytically active complex can be formed less readily under such conditions; indeed the solutions of Ru complexes, which show a characteristic yellow to red transition in catalytically active systems, remained yellow in case of catalysis with pretreated complexes. Unfortunately, these data do not allow deeper elaboration of the molecular events during the induction period of the reaction.

In order to increase the coordination rigidity around the metal ion, some of the complexes were encapsulated inside the cavities of sol–gel glasses in the hope of a further increase in enantioselectivity. However, in addition to the anticipated lower reaction rates due to diffusion barriers, the enantioselectivities decreased as well. This is most probably a consequence of a specific pretreatment of the catalyst in a highly aqueous medium during the preparation of the glasses.

In summary, all the discussed features suggest that, during the induction period, a single active catalyst is formed which is capable of discriminating between the two enantiotopic faces of the substrate. This catalytic species still has some coordination flexibility and is very much influenced by the nature of the aminoacidate ligand. However, on prolonged reaction, it is gradually replaced by either a non-selective metal complex or by a mixture of complexes, the components of which may independently catalyse the selective formation of both enantiomeric alcohols.

Although the mechanism of aldehyde reduction with hydrogen transfer from 2-propanol was not examined in detail, coordination through the carbonyl function would lead to formation of intermediates of the same type as with acetophenone, that is **VI** and **VII**. Weak coordination of the C=C unsaturated bond in α,β-unsaturated aldehydes explains the selectivity towards the formation of the unsaturated alcohol and is in accordance with the lack of isomerisation, both in case of the unsaturated aldehydes and of simple

0947-6539/99/0505-1560 $ 17.50+.50/0 *Chem. Eur. J.* **1999**, *5*, No. 5

olefins, such as allylbenzene. Other steps of the mechanism can also be assumed to be the same as in the case of acetophenone reduction.

Conclusions

A family of trinuclear amino acidate cations $[\{(\eta\text{-ring})M(Aa)\}_3]^{3+}$ can be readily prepared from the corresponding mononuclear chlorides $[(\eta\text{-ring})M(Aa)Cl]$. The stereochemical properties of the new compounds can be studied by judicious combination of X-ray, NMR, and CD measurements. Trimerisation takes place with *chiral self-recognition* to afford exclusively trimers with the same configuration at the three metal atoms. In general, the trimers isomerise in highly polar solvents, the rates of diastereomerisation being strongly metal dependent. These rates increase in the sequence $Ru \ll Ir < Rh$. The different diastereomer stability observed in solution can be qualitatively explained by consideration of the localisation of the polar groups on the molecular surface.

These compounds are highly enantioselective catalysts for the reduction of acetophenone by means of hydrogen transfer from 2-propanol (up to 75% *ee*) and for the selective reduction of α,β-unsaturated aldehydes to α,β-unsaturated alcohols. The reaction requires the presence of a mild base and therefore is also applicable for base-sensitive substrates. The water solubility of the complexes allows their use as catalysts in aqueous/organic biphasic systems.

Experimental Section

General comments: Infrared spectra were recorded on Perkin-Elmer 783 and 1330 spectrophotometers (range 4000–200 cm^{-1}) with Nujol mulls between polyethylene sheets or dichloromethane solutions between NaCl plates. Carbon, hydrogen, and nitrogen analyses were performed with a Perkin-Elmer 240B microanalyser. NMR data were recorded on a Varian UNITY 300 spectrometer operating at 299.95 (^{1}H) and 75.4 (^{13}C) MHz. Chemical shifts are expressed in ppm upfield from $SiMe_4$. Coupling constants J are given in Hertz. Mass spectra were measured on a VG Autospec double-focusing mass spectrometer operating in the FAB^+ mode. Ions were produced with the standard Cs^+ gun at about 30 KV and 3-nitrobenzyl alcohol (NBA) was used as matrix. CD spectra were determined in a 0.1 or 1 cm path length cell with a Jasco-710 apparatus, at concentrations of approximately 5×10^{-3} M. Conductivities were measured with a Philips 9501/01 conductimeter at concentrations from 10^{-4} to 10^{-3} M. Acetophenone and citral were purchased from Aldrich, cinnamaldehyde from Schuchardt and were used as received. Reagent grade 2-propanol was purified with standard methods.

Preparation of the complexes $[\{(\eta\text{-ring})M(Aa)\}_3](BF_4)_3$ (1–9): An equimolar amount of $AgBF_4$ was added to a 0.05 M solution of the corresponding $[(\eta\text{-ring})M(Aa)Cl]$ compound in methanol. The mixture was stirred for 1 h in the absence of light, and the precipitated AgCl was filtered off. The resulting solution was concentrated at reduced pressure to about 2 mL. Addition of Et_2O completed the precipitation of an orange (Rh compounds) or yellow (Ir and Ru compounds) solid which was filtered off, washed with Et_2O, and vacuum-dried. All the ruthenium trimers crystallise with one molecule of water.

1a: Yield: 80%. IR (Nujol): ν(CO) 1545 (vs); ν(NH) 3325 (s), 3280 (s) cm^{-1}; elemental analysis: calcd for $C_{39}H_{63}N_3B_3F_{12}O_6Rh_3$ (%): C 37.8, H 5.1, N 3.4; found: C 37.4, H 5.2, N 3.4; FAB MS: m/z (%): 1152 ($[\{[Rh](Ala)\}_3(BF_4)_2]^+$, 20), 651 ($[\{[Rh](Ala)\}_2]^+$, 67). **1b**: Yield: 91%. IR (Nujol): ν(CO) 1575 (vs); ν(NH) 3320 (s), 3265 (s) cm^{-1}; elemental analysis: calcd for $C_{39}H_{63}N_3B_3F_{12}O_6Ir_3$ (%): C 31.1, H 4.2, N 2.8; found: C 30.7, H 4.4, N 2.6; FAB MS (%): m/z (%): 1420 ($[\{[Ir](Ala)\}_3(BF_4)_2]^+$, 5), 829 ($[\{[Ir](Ala)\}_2]^+$, 60), 416 ($[[Ir](Ala)]^+$, 100); conductivity:[48] (acetone) B = 1647.5. **1c**: Yield: 78%. IR (Nujol): ν(CO) 1575 (vs); ν(NH) 3320 (m) 3280 (m); ν(OH) 3620 (m) cm^{-1}; elemental analysis calcd for $C_{39}H_{62}N_3B_3F_{12}O_7Ru_3$ (%): C 36.5, H 5.2, N 3.3; found: C 36.4, H 5.3, N 3.4; conductivity: (acetone) B = 841.5; (methanol) B = 816.2. **2a**: Yield: 93%. IR (Nujol): ν(CO) 1530 (vs); ν(NH) 3330 (s), 3279 (s) cm^{-1}; elemental analysis calcd for $C_{42}H_{69}N_3B_3F_{12}O_6Rh_3$ (%): C 39.4, H 5.4, N 3.3; found: C 38.8, H 5.4, N 3.3; FAB MS: m/z (%): 1195 ($[\{[Rh](Abu)\}_3(BF_4)_2]^+$, 10), 679 ($[\{[Rh](Abu)\}_2]^+$, 62). **3a**: Yield: 80%. IR (Nujol): ν(CO) 1560 (vs); ν(NH) 3280 (s), 3160 (s) cm^{-1}; elemental analysis calcd for $C_{45}H_{71}N_3B_3F_{12}O_6Rh_3$ (%): C 40.8, H 5.7, N 3.2; found: C 40.3, H 5.7 N 3.4; FAB MS: m/z (%): 1236 ($[\{[Rh](Val)\}_3(BF_4)_2]^+$, 20), 707 ($[\{[Rh](Val)\}_2]^+$, 98), 354 ($[[Rh](Val)]^+$, 100). **3b**: Yield: 74%. IR (Nujol): ν(CO) 1575 (vs); ν(NH) 3340 (s), 3300 (s) cm^{-1}; elemental analysis calcd for $C_{45}H_{71}N_3B_3F_{12}O_6Ir_3$ (%): C 34.0, H 4.8, N 2.6; found: C 33.6, H 4.9, N 2.5; conductivity: (acetone) B = 1632.3. **3c**: Yield: 72%. IR (Nujol): ν(CO) 1570 (vs); ν(NH) 3320 (m), 3280 (m); ν(OH) 3625 (m) cm^{-1}; elemental analysis calcd for $C_{45}H_{70}N_3B_3F_{12}O_7Ru_3$ (%): C 40.6, H 5.6, N 3.1; found: C 40.6, H 5.5, N 3.1. FAB MS: m/z (%): 1229 ($[\{[Ru](Val)\}_3(BF_4)_2]^+$, 7), 702 ($[\{[Ru](Val)\}_2]^+$, 30), 530 $[[Ru](Val)(BF_4)_2]^+$, 15). Conductivity: (acetone) B = 1566.4; (methanol) B = 1134.5. **4a**: Yield: 98%. IR (Nujol): ν(CO) 1565 (vs); ν(NH) 3310 (s), 3260 (s) cm^{-1}; elemental analysis calcd for $C_{48}H_{81}N_3B_3F_{12}O_6Rh_3$ (%): C 42.2, H 6.0, N 3.1; found: C 41.4, H 5.9, N 3.0; FAB MS: m/z (%): 1279 ($[\{[Rh](Tle)\}_3(BF_4)_2]^+$, 5), 736 ($[\{[Rh](Tle)\}_2]^+$, 47), 368 ($[[Rh](Tle)]^+$, 100). **4b**: Yield: 91%. IR (Nujol): ν(CO) 1565 (vs); ν(NH) 3350 (s), 3260 (s) cm^{-1}; elemental analysis calcd for $C_{48}H_{81}N_3B_3F_{12}O_6Ir_3$ (%): C 35.3, H 5.0, N 2.6; found: C 35.8, H 4.6, N 2.5; FAB MS: m/z (%): 1546 ($[\{[Ir](Tle)\}_3(BF_4)_2]^+$, 2), 915 ($[\{[Ir](Tle)\}_2]^+$, 12), 458 ($[[Ir](Tle)]^+$, 100). **4c**: Yield: 78%. IR (Nujol): ν(CO) 1570 (vs); ν(NH) 3290 (m); ν(OH) 3590 (m) cm^{-1}; elemental analysis calcd for $C_{48}H_{80}N_3B_3F_{12}O_7Ru_3$ (%): C 41.9, H 5.9, N 3.0; found: C 41.7, H 5.8; N 3.0; conductivity: (acetone) B = 773.2; (methanol) B = 610.0. **5a**: Yield: 79%. IR (Nujol): ν(CO) 1575 (vs); ν(NH) 3320 (s), 3270 (s) cm^{-1}; elemental analysis calcd for $C_{57}H_{75}N_3B_3F_{12}O_6Rh_3$(%): C 46.7, H 5.2, N 2.9; found: C 46.0, H 5.0, N 2.8; FAB MS: m/z (%): 1380 ($[\{[Rh](Phe)\}_3(BF_4)_2]^+$, 12), 803 ($[\{[Rh](Phe)\}_2]^+$, 57). **5b**: Yield: 80%. IR (Nujol): ν(CO) 1575 (vs); ν(NH) 3310 (s), 3270 (s) cm^{-1}; elemental analysis calcd for $C_{57}H_{75}N_3B_3F_{12}O_6Ir_3$ (%): C 39.5, H 4.4, N 2.4; found: C 39.0, H 4.4, N 2.3; FAB MS: m/z (%): 1648 ($[\{[Ir](Phe)\}_3(BF_4)_2]^+$, 3), 981 ($[\{[Ir](Phe)\}_2]^+$, 44), 492 ($[[Ir](Phe)]^+$, 100). **5c**: Yield: 72%. IR (Nujol): ν(CO) 1590 (vs); ν(NH) 3340 (m), 3290 (m); ν(OH) 3625 (m) cm^{-1}; elemental analysis calcd for $C_{57}H_{74}N_3B_3F_{12}O_7Ru_3$ (%): C 46.4, H 5.0, N 2.9; found: C 46.5, H 4.9, N 2.9; FAB MS: m/z (%): 1373 ($[\{[Ru](Phe)\}_3(BF_4)_2]^+$, 5), 799 ($[\{[Ru](Phe)\}_2]^+$, 38), 400 $[[Ru](Phe)]^+$, 44); conductivity: (acetone) B = 695.1; (methanol) B = 412.3. **6a**: Yield: 82%. IR (Nujol): ν(CO) 1580 (vs); ν(NH) 3270 (s) cm^{-1}; elemental analysis calcd for $C_{45}H_{69}N_3B_3F_{12}O_6Rh_3$ (%): C 41.0, H 5.3, N 3.2; found: C 40.5, H 5.4, N 3.4; FAB MS: m/z (%): 1230 ($[\{[Rh](Pro)\}_3(BF_4)_2]^+$, 18), 703 ($[\{[Rh](Pro)\}_2]^+$, 100), 352 ($[[Rh](Pro)]^+$, 78). **6b**: Yield: 65%. IR (Nujol): ν(CO) 1575 (vs); ν(NH) 3260 (s) cm^{-1}; elemental analysis calcd for $C_{45}H_{69}N_3B_3F_{12}O_6Ir_3$ (%): C 34.1, H 4.4, N 2.7; found: C 33.8, H 4.5, N 2.4; FAB MS: m/z (%): 1498 ($[\{[Ir](Pro)\}_3(BF_4)_2]^+$, 2), 881 ($[\{[Ir](Pro)\}_2]^+$, 56), 442 ($[[Ir](Pro)]^+$, 100); conductivity: (acetone) B = 1729.0; **6c**: Yield: 71%. IR (Nujol): ν(CO) 1580 (vs); ν(NH) 3285 (m); ν(OH) 3620 (m) cm^{-1}; elemental analysis calcd for $C_{45}H_{68}N_3B_3F_{12}O_7Ru_3$ (%): C 40.8, H 5.2, N 3.2; found: C 41.0, H 5.1, N 3.2; FAB MS: m/z (%): 1222 ($[\{[Ru](Pro)\}_3(BF_4)_2]^+$, 10), 698 ($[\{[Ru](Pro)\}_2]^+$, 36), 350 $[[Ru](Pro)]^+$, 40); conductivity: (acetone) B = 1036.1; (methanol) B = 1012.9. **7a**: Yield: 88%. IR (Nujol): ν(CO) 1580 (vs); ν(NH) 3270 (s) cm^{-1}; elemental analysis calcd for $C_{45}H_{69}N_3B_3F_{12}O_6Rh_3$ (%): C 41.0, H 5.3, N 3.2; found: C 40.7, H 5.2, N 3.3. **7b**: Yield: 80%. IR (Nujol): ν(CO) 1575 (vs); ν(NH) 3260 (s) cm^{-1}; elemental analysis calcd for $C_{45}H_{69}N_3B_3F_{12}O_6Ir_3$ (%): C 34.1, H 4.4, N 2.7; found: C 33.7, H 4.7, N 2.5; FAB MS: m/z (%): 1498 ($[\{[Ir](Pro)\}_3(BF_4)_2]^+$, 4), 881 ($[\{[Ir](Pro)\}_2]^+$, 30), 442 ($[[Ir](Pro)]^+$, 100). **7c**: Yield: 71%. IR (Nujol): ν(CO) 1580 (vs); ν(NH) 3285 (m); ν(OH) 3620 (m) cm^{-1}. Elemental analysis calcd for $C_{45}H_{68}N_3B_3F_{12}O_7Ru_3$ (%): C 40.8, H 5.2, N 3.2; found: C 40.5, H, 5.1, N 3.4; conductivity: (acetone) B = 1199.0; (methanol) B = 886.7. **8a**: Yield: 87%. IR (Nujol): ν(CO) 1565 (vs) cm^{-1}; elemental analysis calcd for $C_{48}H_{75}N_3B_3F_{12}O_6Rh_3$ (%): C 42.4, H 5.6, N 3.1; found: C 42.2, H 5.4, N 3.0; FAB MS: m/z (%): 1272 ($[\{[Rh](Me\text{-}Pro)\}_3(BF_4)_2]^+$, 8), 732 ($[\{[Rh](Me\text{-}Pro)\}_2]^+$, 38), 366 ($[[Rh](Me\text{-}pro)]^+$, 89). **8b**: Yield: 82%. IR

(Nujol): ν(CO) 1560 (vs) cm^{-1}; elemenetal analysis calcd for $C_{48}H_{75}N_3B_3F_{12}O_6Ir_3$ (%): C 35.4, H 4.7, N 2.6; found: C 35.1, H 4.3, N 2.4; FAB MS: *m*/*z* (%): 1540 ([{[Ir](Me-Pro)}$_3$(BF$_4$)$_2$]$^+$, 2), 912 ([{[Ir](Me-Pro)}$_2$]$^+$, 7), 456 ([[Ir](Me-Pro)]$^+$, 100); conductivity: (acetone) B = 1555.4. **9a**: Yield: 90%. IR (Nujol): ν(CO) 1565 (vs); ν(NH) 3300 (m) cm^{-1}; elemental analysis calcd for $C_{45}H_{69}N_3B_3F_{12}O_9Rh_3$ (%): C 39.6, H 5.1, N 3.1; found: C 40.1, H 5.2, N 3.3; FAB MS: *m*/*z* (%): 1278 ([{[Rh](Hyp)}$_3$(BF$_4$)$_2$]$^+$, 12), 735 ([{[Rh](Hyp)}$_2$]$^+$, 100), 368 ([[Rh](Hyp)]$^+$, 80). **9b**: Yield: 86%. IR (Nujol): ν(CO) 1575 (vs); ν(NH) 3250 (m) cm^{-1}; elemental analysis calcd for $C_{45}H_{69}N_3B_3F_{12}O_7Ir_3$(%): C 33.1, H 4.3, N 2.6; found: C 32.7, H 4.3, N 2.5. **9c**: Yield: 73%. IR (Nujol): ν(CO) 1557 (vs); ν(NH) 3280 (m); ν(OH) 3615 (m) cm^{-1}; elemental analysis calcd for $C_{45}H_{68}N_3B_3F_{12}O_8Ru_3$ (%): C 46.4, H 5.0, N 2.9; found: C 46.5, H 4.9, N 2.9; FAB MS: *m*/*z* (%): 1270 ([{[Ru](Hyp)}$_3$(BF$_4$)$_2$]$^+$, 24), 731 ([{[Ru](Hyp)}$_2$]$^+$, 90), 366 [[Ru](Hyp)]$^+$, 90); conductivity: (acetone) B = 1142.6; (methanol) B = 722.5.

X-ray structure analysis of 1b and 6c·3CH$_3$OH: Crystals were obtained by slow diffusion of diethyl ether into methanolic solutions of the complexes. The orientation matrix and unit cell dimensions were determined by least-squares fit from a set of high-angle, carefully centred, reflections (40 for **1b**, and 25 for **6c**) on a Siemens-Stoe AED-2 four-circle diffractometer with graphite-monochromated $Mo_{K\alpha}$ radiation (λ = 0.71073 Å). Data collection for both crystals was carried out with the $\omega/2\theta$ scan technique to a maximum of 45 (**1b**) or 47° (**6c**). Three standard reflections were measured every hour as a check on crystal and instrument stability. A linear correction based on these standards was applied to account for the intensity decay. All data were corrected for absorption, Lorentz and polarisation effects. In the case of **1b**, a semi-empirical method was applied for the absorption correction;[49] for **6c** the best results were obtained with an empirical approach[50] (see Table 9). Both structures were solved by standard Patterson and difference Fourier methods.[51] The positions and anisotropic thermal parameters of all non-hydrogen atoms were refined satisfactorily by full-matrix least-squares calculations (SHELXL-93 program[52]) except those of the disordered tetrafluoroborate anion in **1b**. In this crystal, the BF_4 anions occupied two different zones of the asymmetric unit with, in both cases, a spherical distribution of the electron density. In both spatial regions, the anions were observed to be statically disordered and were modelled on the basis of two groups of atoms in each case, including complementary occupancy factors (0.52(3) for B(1), F(1a), F(2a); 0.22(3) for B(2), F(1b), F(2b); 0.37(3) for B(3), F(1c)–F(4c); 0.38(3) for B(4), F(1d)–F(4d)) and restrained positional and thermal parameters. The BF_4 anions in **6c** also showed a large dispersion of their electron density; however, no clear model of static disorder could be established and, eventually, dynamic disorder was assumed. Hydrogen coordinates were found in difference Fourier maps for those atoms bonded to the chiral centres of the aminoacidate ligands (N(1) and C(2)); all the remaining atoms were included in both structures at their ideal positions. All hydrogen atoms were refined riding at their C or N atoms with one (**1b**) or six (**6c**) common thermal parameters. The absolute structure was checked in both structures by the estimation of the Flack parameter *x* in the final cycles of refinement, 0.00(3) (**1b**) and 0.04(7) (**6c**).[53] Final agreement parameters are collected in Table 9, together with some crystallographic data and additional experimental details. Crystallographic data (excluding structure factors) for the structures reported in this paper have been deposited with the Cambridge Crystallographic Data Center as supplementary publication nos. CCDC-10218 (**1b**) and CCDC-102219 (**6c**). Copies of the data can be obtained free of charge on application to CCDC, 12 Union Road, Cambridge CB21EZ, UK (fax: (+44) 1223-336-033; e-mail: deposit@ccdc.cam.ac.uk).

Transfer hydrogenation experiments, standard reaction conditions: Catalyst (0.01 mmol metal), base (0.02 mmol; as 100 μL 0.2 M aqueous solution), acetophenone (0.25 mL, 2.14 mmol) or citral (1.46 mmol), 2-propanol (5 mL), reflux (83 °C), argon atmosphere. In experiments with cinnamaldehyde (0.25 mL, 2.0 mmol) solid HCOONa (3.4 mg, 0.05 mmol) was used instead of the aqueous solution. All the components of the reaction were mixed under argon at room temperature in a Schlenk tube which was then equipped with a reflux condenser and immersed to an oil bath of 83 °C after complete dissolution of the solid complex. The mixture was stirred magnetically and a slow argon flow (5–8 bubbles per min) was maintained through the tube during the reaction. The reactions were monitored by gas-liquid chromatography (HP-Innowax column, 30 M, i.d. 0.53 mm, film thickness 1.0 μm, 140 °C, isotherm, FID, carrier: He) and the products were identified by their retention times compared to those of authentic samples. Enantiomeric composition of the product 1-phenylethanol was determined using a Cyclodextrin column (CP-Cyclodex-B 236-M, 50 m × 0.25 mm × 0.25 μm film, 110 °C)

Immobilisation by the sol–gel method followed the procedure given in ref [35].

Acknowledgments

We thank the Dirección General de Investigación Científica y Técnica for financial support (Grant PB96/0845). F. J. is grateful to IBERDROLA S.A. for sponsoring a visiting professorship at the Department of Inorganic Chemistry, University of Zaragoza during the fall semester, 1995/96 and Á. K. acknowledges the travel grant of the European Community in the framework of the project Catalysis by Metal Complexes involving Small Molecules (ERBCHRXCT930147). We are also grateful to Dr. David L. Davies for his comments on the nature of the ruthenium species.

[1] a) R. Krämer, K. Polborn, H. Wanjek, I. Zahn, W. Beck, *Chem. Ber.* **1990**, *123*, 767; b) D. Carmona, A. Mendoza, F. J. Lahoz, L. A. Oro, M. P. Lamata, E. San José, *J. Organomet. Chem.* **1990**, *396*, C17.

Table 9. Crystallographic data and structure refinement for **1b** and **6c**·3CH$_3$OH.

	1b	**6c**
formula	$C_{39}H_{63}B_3F_{12}Ir_3N_3O_6$	$C_{45}H_{66}B_3F_{12}N_3O_6Ru_3\cdot 3CH_3OH$
M_r	1506.95	1404.77
crystal size	0.31 × 0.22 × 0.20	0.49 × 0.38 × 0.34
crystal system	hexagonal	orthorhombic
space group	$P6_3$ (no. 173)	$P2_12_12_1$ (no. 19)
a [Å]	17.3702(8)	15.387(2)
b [Å]	17.3702(8)	19.142(6)
c [Å]	10.8263(13)	20.045(3)
V [Å^3]	2828.9(4)	5904(2)
Z	2	4
ρ_{calcd} [g cm^{-3}]	1.769	1.580
T [K]	293(2)	173.0(2)
μ [mm^{-1}]	7.118	0.848
2θ range data collec. [°]	4–45	3–47
index ranges	$0 \le h \le 16$, $-18 \le k \le 18$, $0 \le l \le 11$ $-16 \le h \le 0$, $-18 \le k \le 0$, $-11 \le l \le 0$	$0 \le h \le 17$, $0 \le k \le 21$, $0 \le l \le 22$ $-17 \le h \le 1$, $-21 \le k \le 1$, $-22 \le l \le 0$
no. measd refls	6048	10379
no. unique refls	2468 (R_{int} = 0.0390)	8654 (R_{int} = 0.0496)
absorption correction method	ψ-scan	empirical
min., max. trans. factors	0.419, 0.469	0.568, 1.000
data/restraints/param	2467/38/210	8642/210/724
$R(F)$ [$F^2 > 2\sigma(F^2)$][a]	0.0380 (1854 refls)	0.0598 (7599 refls)
$wR(F^2)$ [all data][b]	0.0987[c]	0.1778[c]
S [all data][b]	1.059[c]	1.141

[a] $R(F) = \Sigma||F_o| - |F_c||/\Sigma|F_o|$. [b] $wR(F^2) = (\Sigma[w(F_o^2 - F_c^2)^2]/\Sigma[w(F_o^2)^2])^{1/2}$. [c] $w = 1/[\sigma^2(F_o^2) + (aP)^2 + bP]$ with $P = (F_o^2 + 2F_c^2)/3$; a = 0.0551 and b = 0 for **1b**, and a = 0.0630 and b = 56.5709 for **6c**. [d] $S = [\Sigma[w(F_o^2 - F_c^2)^2]/(n - p)]^{1/2}$; n = number of reflections, p = number of parameters.

[2] a) D. F. Dersnah, M. C. Baird, *J. Organomet. Chem*. **1977**, *127*, C55; b) W. S. Sheldrick, S. Heeb, *Inorg. Chim. Acta* **1990**, *168*, 93.

[3] The experimental values for the coefficients B in the Onsager equation $\Lambda_{eq} = \Lambda_0 - Bc^{1/2}$ were 348.5 (M = Rh, Aa = Ala), 622.5 (M = Ir, Aa = Ala), 347.8 (M = Rh, Aa = L-Pro), and 627.9 (M = Ir, Aa = L-Pro). a) R. D. Feltham, R. G. Hayter, *J. Chem Soc*. **1964**, 4587; b) W. J. Geary, *Coord. Chem. Rev.* **1971**, *7*, 81.

[4] R. Krämer, K. Polborn, C. Robl, W. Beck, *Inorg. Chim. Acta* **1992**, *198–200*, 415.

[5] a) *Aqueous Organometallic Chemistry and Catalysis.* (Eds.: I. T. Horváth, F. Joó) NATO ASI Series: High Technology, *Vol. 5,* Kluwer, Dordrecht, **1995**; b) *Aqueous Organometallic Catalysis - Principles and Applications* (Eds.: B. Cornils, W. A. Herrmann), WILEY-VCH, Weinheim, **1998**; c) *Catalysis in Water* (Ed.: I. T. Horváth) Special issue of *J. Mol. Catal. A* **1995**, *116*; d) F. Joó, J. Kovács, A.Cs. Bényei, Á. Kathó, *Angew. Chem.* **1998**, *110*, 1024; *Angew. Chem. Int. Ed.* **1998**, *37*, 969.

[6] a) P. A. Chaloner, M. A. Esteruelas, F. Joó, L. A. Oro, *Homogeneous Hydrogenation (Catalysis by Metal Complexes*, *Vol 15),* Kluwer, Dordrecht, **1994**; b) R. Noyori, S. Hashiguchi, *Acc. Chem. Res.* **1997**, *30*, 97; c) T. Langer, G. Helmchen, *Tetrahedron Let.* **1996**, *37*, 1381.

[7] a) S. Hashiguchi, A. Fujii, J. Takehara, T. Ikariya, R. Noyori, *J. Am. Chem. Soc.* **1995**, *117*, 7562; b) R. L. Chowdhury, J.-E. Bäckvall, *J. Chem. Soc. Chem. Commun*. **1991**, 1063; c) P. Kvintovics, B. R. James, B. Heil, *J. Chem. Soc. Chem. Commun*. **1986**, 1810; d) J.-X. Gao, T. Ikariya, R. Noyori, *Organometallics*, **1996**, *15*, 1087; e) P. Krasik, H. Alper, *Tetrahedron*, **1994**, *50*, 4347.

[8] a) L. A. Oro, D. Carmona, J. Reedijk, *Inorg. Chim. Acta* **983**, *71*, 115; b) L. A. Oro, D. Carmona, M. P. Lamata, A. Tiripicchio, F. J. Lahoz, *J. Chem. Soc. Dalton Trans.* **1986**, 15.

[9] C. J. Jones, J. A. McCleverty, A. S. Rothin, *J. Chem. Soc. Dalton Trans.* **1986**, 109.

[10] K. Nakamoto, *Infrared and Raman Spectra of Inorganic and Coordination Compounds*, 4th ed., Wiley-Interscience, New York, **1986**, p. 132.

[11] W. S. Sheldrick, R. Exner, *Inorg. Chim. Acta* **1989**, *166*, 213.

[12] The sequence rules establish the following priority order: η-ring > O quelate > O bridging > N. See: a) R. S. Cahn, C. Ingold, V. Prelog, *Angew. Chem.* **1966**, *78,* 413, *Angew. Chem. Int. Ed. Engl.* **1966**, *4*, 385; b) V. Prelog, G. Helmchen, *Angew. Chem.* **1982**, *94*, 614, *Angew. Chem. Int. Ed. Engl.* **1982**, *21*, 576; c) C. Lecomte, Y. Dusausoy, J. Protas, J. Tirouflet, *J. Organomet. Chem*. **1974**, *73*, 67; d) K. Stanley, M. C. Baird, *J. Am. Chem. Soc*. **1975**, *97*, 6599; e) T. E. Sloan, *Top. Stereochem*. **1981**, *12*, 1.

[13] A detailed search of 'M(pro)' fragments in the CSD file showed all the structures to have identical chirality for the α-carbon and for the coordinated aminic nitrogen of the aminoacidate ligand. See also: a) R. D. Gillard, O. P. Slyudkin, *J. Chem. Soc. Dalton Trans.* **1978**, 152; b) H. Kollowski, L. D. Pettit in *Chemistry of the Platinum Group Metals* (Ed.: F. R. Hartley), Elsevier, New York, **1991**, Ch. 15, p. 530.

[14] R. Atencio, PhD Thesis, University of Zaragoza, **1995**, Zaragoza.

[15] The configuration around the metal centre in $[\{(\eta^5\text{-}C_5Me_5)\text{-}Rh(Phe)\}_3]^{3+}$ is identical to that observed in **1b**, but the chiral descriptors assigned in the original paper[4] are opposite: $S_{Rh}S_{Rh}S_{Rh}$.

[16] I. Zahn, K. Polborn, B. Wagner, W. Beck, *Chem. Ber.* **1991**, *124*, 1065.

[17] D. Carmona, F. J. Lahoz, R. Atencio, L. A. Oro, M. P. Lamata, E. San José, *Tetrahedron Asymmetry* **1993**, *4*, 1425.

[18] D. B. Grotjahn, C. Joubran, J. L. Hubbard, *Organometallics* **1996**, *15*, 1230.

[19] F. H. Allen, J. E. Davies, J. J. Galloy, O. Johnson, O. Kennard, C. F. Macrae, E. M. Mitchell, G. F. Mitchell, J. M. Smith, D. G. Watson *J. Chem. Inf. Comput. Sci.* **1991**, *31*, 187.

[20] For the D-prolinate compounds **7** the configurations at the carbon and nitrogen atoms are *R*. The configuration at the HC(OH) carbon of the 4-OH-L-prolinate complexes **9** is *R* and it is not quoted in the general descriptors.

[21] The term trimer molecule in this analysis refers to a set of atoms that include all the crystallographically independent atoms of the trinuclear complex and those of only one of the two disordered BF_4 groups (B(3), F(1c)–F(4c)).

[22] a) A. J. Pertsin, A. Kitaigorodski, *The Atom-Atom Potential Method*, Springer, Berlin, **1987**; b) A. Gavezzotti, M. Simonetta, *Organic Solid State Chemistry* (Ed.: G. R. Desiraju), Elsevier, Amsterdam, **1987**.

[23] The method applied is analogous to that described in: a) D. Braga, F. Grepioni, P. Sabatino, *J. Chem. Soc. Dalton Trans.* **1990**, 3137; b) D. Braga, F. Grepioni, *Organometallics* **1991**, *10*, 1254.

[24] A. Gavezzotti, *OPEC*, *Organic Packing Potential Energy Calculations.* University of Milano, Italy, **1987**. See also: A. Gavezzotti, *J. Am. Chem. Soc.* **1983**, *95*, 5220.

[25] The tetrafluoroborate trimers are almost insoluble in $CHCl_3$, Et_2O, and hydrocarbon solvents. Due to solubility reasons we were not able to carry out solution measurements for the following solvent/complex pairs: in dichloromethane, acetone, methanol, and water, compounds **1a**, **2a**, **9a**, and **9b**; in dichloromethane, methanol, and water, compounds **3a** and **5a**; in dichloromethane, compounds **1c**, **3c**, **4b**, and **9c**; in methanol and water, compound **3b** and in water, compounds **4c** and **5b**.

[26] The composition of the mixtures was obtained by careful integration of the corresponding C_5Me_5 (rhodium and iridium trimers) or methyl arene protons (ruthenium derivatives) of each diastereomer. Error limits in each integral are estimated as ±2%.

[27] The CD and some NOEDIFF spectra of the rhodium trimers are included as supplementary material.

[28] Again, the L-prolinate complexes **6a**,**b** behaved differently, the amount of the ρ diastereomer increasing with time.

[29] Diastereomeric compositions for the iridium trimers **3b**, **4b**, **6b**, and **8b** are included in the supplementary material.

[30] R. G. Wilkins, *Kinetics and Mechanism of Reactions of Transition Metal Complexes* (2nd ed), VCH, Weinheim, **1991**, p. 13.

[31] Recently, Fish et al. reported that only the σ diastereomer of the phenyl alaninate rhodium trimer $[\{(\eta^5\text{-}C_5Me_5)Rh(Phe)\}_3](BF_4)_3$ (**5a**) was present in D_2O (pD, 6) from 5 to 65 °C: S. Ogo, H. Chen, M. M. Olmstead, R. H. Fish, *Organometallics* **1996**, *15*, 2009.

[32] Surprisingly, the diastereomerisation of the iridium compound **8b** in water was accompanied by partial deuteration of the N–Me amino acidate group. We have no satisfactory explanation for this.

[33] D. G. McCollum, C. Fraser, R. Ostrander, A. L. Rheingold, B. Bosnich, *Inorg. Chem.* **1994**, *33*, 2383.

[34] Obviously, for the D-prolinate compound **7c** the corresponding enantiomers of the L-prolinate **6c** were observed in each case, as assayed by CD spectroscopy.

[35] a) H. Shertchook, D. Avnir, J. Blum, F. Joó, Á. Kathó, H. Schumann, R. Weimann, S. Wernik, *J. Mol. Catal. A*, **1996**, *108*, 153; b) A. Rosenfeld, D. Avnir, J. Blum, *J. Chem. Soc. Chem. Commun.* **1993**, 583; c) D. Avnir, S. Braun, M. Ottolenghi, *Am. Chem. Soc. Symp. Ser.* **1992**, *499*, 384.

[36] E. L. Eliel, S. H. Wilen, L. N. Mander, *Stereochemistry of Organic Compounds,* Wiley-Interscience, New York, **1994**, p. 365.

[37] For recently reported organometallic examples see: a) H. Brunner, R. Oeschey, B. Nuber, *J. Chem. Soc. Dalton Trans.* **1996**, 1499; b) H. Brunner, R. Oeschey, B. Nuber, *Organometallics* **1996**, *15*, 3616.

[38] T. Ohkuma, H. Ooka, T. Ikariya, R. Noyori, *J. Am. Chem. Soc.* **1995**, *117*, 10417.

[39] a) F. Joó, A. Bényei, *J. Organomet. Chem*. **1989**, *363*, C19; b) A. Bényei, F. Joó, *J. Mol. Catal*. **1990**, *58*, 151; c) D. J. Darensbourg, F. Joó, M. Kannisto, Á. Kathó, J. H. Reibenspies, D. J. Daigle, *Inorg. Chem.* **1994**, *33*, 200; d) D. J. Darensbourg, F Joó, M. Kannisto, Á. Kathó, J. H. Reibenspies, *Organometallics* **1992**, *11*, 1992.

[40] a) G. Allmang, F. Grass, J. M. Grosselin, C. Mercier, *J. Mol. Catal.* **1991**, *66*, L27; b) J. M. Grosselin, C. Mercier, G. Allmang, F. Grass, F. *Organometallics* **1991**, *10*, 2126.

[41] a) G. Zassinovich, G. Mestroni, S. Gladiali, *Chem. Rev.* **1992**, *92*, 1051; b) G.-Z. Wang, J.-E. Bäckvall, *J. Chem. Soc. Chem. Commun*. **1992**, 980; c) Z. Yuskovetz, M. Shimanska, *Khim. Geterocikl. Soed.* **1994**, 435; d) M. Palmer, T. Walsgrove, M. Wills, *J. Org. Chem*. **1997**, *62*, 5226; e) D. A. Alonso, D. Guijarro, P. Pinho, O. Temme, P. G. Andersson, *J. Org. Chem.* **1998**, *63*, 2749; f) L. Schwink, T. Ireland, K. Püntener, P. Knochel, *Tetrahedron: Asymmetry.* **1998**, *9*, 1143; g) C. Bianchini, L. Glendenning, F. Zanobini, E. Farnetti, M. Graziani, E. Nagy, *J. Mol. Catal. A*. **1998**, *132*, 13.

[42] E. Mizushima, M. Yamaguchi, T.Yamagishi, *Chem. Let.* **1997**, 237.

[43] T. Ohkuma, H. Ooka, S. Hashiguchi, T. Ikariya, R. Noyori, *J. Am. Chem. Soc.* **1995**, *117*, 2675.

[44] H. Yang, M. Alvarez, N. Lugan, R. Mathieu, *J. Chem. Soc. Chem. Commun*. **1995**, 1721.

[45] a) J. W. Kang, P. M. Maitlis, *J. Organomet. Chem.* **1971**, *30*, 127; b) C. White, A. J. Oliver, P. M. Maitlis, *J. Chem. Soc. Dalton Trans.* **1973**, 1901; c) A. Nutton, P. M. Bailey, P. M. Maitlis, *J. Chem. Soc. Dalton Trans.* **1981**, 1997; d) A. Nutton, P. M. Maitlis, *J. Chem. Soc. Dalton Trans.* **1981**, 2339; e) D. Carmona, L. A. Oro, M. P. Lamata, M. P. Puebla, J. Ruiz, P. M. Maitlis, *J. Chem. Soc. Dalton Trans.* **1987**, 639; f) T. Arthur, D. R. Robertson, D. A. Tocher, T. A. Stephenson, *J. Organomet. Chem*. **1981**, *208*, 389.

[46] a) J. W. Kang, K. Moseley, P. M. Maitlis, *J. Am. Chem. Soc*. **1969**, *91*, 5970; b) D. Carmona, F. J. Lahoz, L. A. Oro, M. P. Lamata, F. Viguri, E. San José, *Organometallics* **1996**, *15*, 2961.

[47] K.-J. Haack, S. Hashiguchi, A. Fujii, T. Ikariya, R. Noyori, *Angew. Chem.* **1997**, *109*, 297; *Angew. Chem. Int. Ed. Engl.* **1997**, *36*, 285.

[48] B represents the coefficient in the Onsager equation $\Lambda_{eq} = \Lambda_0 - Bc^{1/2}$ where Λ_{eq} is the equivalent conductance, Λ_0 the extrapolated equivalent conductance at zero concentration and c represents the equivalent concentration of the solution.

[49] A. C. T. North, D. C. Phillips, F. S. Mathews, *Acta Crystallogr. Sect. A* **1968**, *24*, 351.

[50] N. Walker, D. Stuart, *Acta Crystallogr. Sect. A* **1983**, *39*, 158.

[51] G. M. Sheldrick, SHELXS-86, program for crystal structure solution, University of Göttingen, Germany, **1990**.

[52] G. M. Sheldrick, SHELXL-93, program for crystal structure refinement, University of Göttingen, Germany, **1993**.

[53] H. D. Flack, *Acta Crystallogr. A* **1983**, *39*, 876.

Received: August 11, 1998 [F 1300]

  0947-6539/99/0505-1564 $ 17.50+.50/0